

**DEVELOPMENT OF NOVEL IMPEDIMETRIC ASSAYS FOR
RAPID DETECTION OF *E. COLI***

By

Vena N. Haynes

B.S. in Biology

Pacific University, 2010

A THESIS

Presented to the

Institute of Environmental Health,

Division of Environmental and Biomolecular Systems

Oregon Health & Science University

School of Medicine

in partial fulfillment of

the requirements for the degree of

Master of Science

in

Environmental Science & Engineering

August 2013

CERTIFICATE OF APPROVAL

This is to certify that the M.S. thesis of
Vena N. Haynes
has been approved

Dr. Holly M. Simon, Associate Professor
Research Advisor

Dr. Richard L. Johnson, Professor

Dr. Ashlee V. Moses, Associate Professor OHSU VGTI
External Examiner

ACKNOWLEDGEMENTS

I would never have been able to finish my thesis without the guidance from my committee members and support from my friends and family.

I would like to express my gratitude towards my research advisor, Dr. Holly Simon, for her guidance, patience and for providing me with an excellent research opportunity. I would like to thank my mentor at Sharp Laboratories of America, Dr. Andrei Ghindilis, for his support, encouragement and vision for my thesis project. I would like to express my appreciation for my research mentor at OHSU, Dr. Mariya Smit, for introducing me to the world of molecular biology as a summer intern prior to my graduate work and for her continual support and patience throughout my graduate work.

I would like to express my gratitude towards Dr. Richard Johnson for participating in my examination committee and to Dr. Ashlee Moses for serving as my external examiner. I would also like to acknowledge Carmen Campbell, Mike Frasier and Kevin Schwarzkopf from SLA for their help with my research and Dr. Lydie Herfort for her useful suggestions and willingness to help.

Acknowledgements go out to Mouzhong Xu for being a wonderful lab-mate and for her endless assistance. I would also like to thank my summer intern Ma'Chesha Banks for her contribution to the research done in Chapter 4 of this thesis. Special thanks goes to all of my CMOP/OHSU friends- my thesis could not have happened without their encouragement, friendship and laughs.

Lastly, I would like to thank my family and friends outside of school for guiding me through difficult times and celebrating in good times, and my dog Bella for always welcoming me home with her wagging tail and kisses.

TABLE OF CONTENTS

ACKNOWLEDGEMENTS.....	iii
TABLE OF CONTENTS.....	iv
LIST OF TABLES AND FIGURES.....	vi
1. Introduction.....	1
2. Genomic DNA-based Assay Development.....	6
2.1 Introduction.....	6
<i>2.1.1 Environmental monitoring.....</i>	<i>6</i>
<i>2.1.2 Impedimetric biosensors.....</i>	<i>6</i>
<i>2.1.3 DNA-based detection.....</i>	<i>7</i>
<i>2.1.4 Aims of this study.....</i>	<i>8</i>
2.2 Materials and Methods.....	8
<i>2.2.1 Sensor arrays.....</i>	<i>8</i>
<i>2.2.2 Array fabrication and functionalization.....</i>	<i>9</i>
<i>2.2.3 Instrumentation.....</i>	<i>9</i>
<i>2.2.4 DNA target preparation.....</i>	<i>9</i>
<i>2.2.5 Sensor array assays.....</i>	<i>10</i>
<i>2.2.6 Data analysis program.....</i>	<i>11</i>
<i>2.2.7 Assay optimization.....</i>	<i>11</i>
2.3 Results and Discussion.....	12
<i>2.3.1 Gene-based detection of dsDNA targets.....</i>	<i>12</i>
<i>2.3.2 Assay optimization.....</i>	<i>13</i>
3. Universal Sensor Array.....	25
3.1 Introduction.....	25
<i>3.1.1 User-friendly technology.....</i>	<i>25</i>
<i>3.1.2 Detection of RNA targets.....</i>	<i>25</i>
<i>3.1.3 Aims of this study.....</i>	<i>26</i>
3.2 Materials and Methods.....	27
<i>3.2.1 DNA target preparation.....</i>	<i>27</i>
<i>3.2.2 Array functionalization.....</i>	<i>28</i>

3.2.3 <i>Sensor array assays and optimization</i>	28
3.3 Results and Discussion	29
3.3.1 <i>Gene-based detection using ssDNA</i>	29
3.3.2 <i>Assay optimization</i>	30
4. Enhancement of assay specificity	42
4.1 Introduction	42
4.1.1 <i>Competition on array surface</i>	42
4.1.2 <i>Enhancing assay specificity</i>	43
4.1.3 <i>Aims of this study</i>	43
4.2 Materials and Methods	44
4.2.1 <i>Multiple probes</i>	44
4.2.2 <i>DNA target preparation</i>	44
4.2.3 <i>Hybridization and optimization using multiple probes</i>	45
4.2.4 <i>Temperature control system</i>	45
4.2.5 <i>Melting curve assays</i>	46
4.3 Results and Discussion	47
4.3.1 <i>Multiple probes improve assay specificity</i>	47
4.3.2 <i>Optimized multiple probe assays</i>	47
4.3.3 <i>Melting curve analysis</i>	49
5. Conclusions and Future Directions	59
5.1 <i>Genomic DNA-based assay development</i>	59
5.2 <i>Universal sensor array</i>	60
5.3 <i>Enhancement of assay specificity</i>	61
6. References	64

List of Tables and Figures

Chapter 2:

Table 2.1	Probe sequences.....	16
Table 2.2	PCR primers.....	17
Table 2.3	Target sequences.....	18
Table 2.4	Gene-based assay optimization.....	19
Figure 2.1	SLA Impedance sensor array.....	20
Figure 2.2	<i>Adk</i> assay optimization.....	21
Figure 2.3	<i>Adk</i> detection limit.....	22
Figure 2.4	<i>Stx</i> assay optimization.....	23
Figure 2.5	<i>Hly</i> assay optimization.....	24

Chapter 3:

Figure 3.1	Assay functionalization.....	33
Figure 3.2	ssDNA target preparation.....	34
Figure 3.3	QC fluorescence.....	35
Figure 3.4	<i>Adk</i> assay diagram.....	36
Figure 3.5	<i>Adk</i> hybridization assay.....	37
Figure 3.6	Idealized assay response.....	38
Figure 3.7	Alternative assay responses.....	39
Figure 3.8	Assay with optimized frequency.....	40
Figure 3.9	<i>Adk</i> assay optimization.....	41

Chapter 4:

Figure 4.1	Multiple probe functionalization techniques.....	51
Figure 4.2	Data analysis algorithm.....	52
Figure 4.3	Amplitude of <i>adk</i> :probe binding.....	53
Figure 4.4	Exponential decay rate of <i>adk</i> :probe binding.....	54
Figure 4.5	Binding rate and integrated area of <i>adk</i> :probe binding.....	55
Figure 4.6	Idealized melting curve.....	56
Figure 4.7	Melting curves associated with increasing temperature.....	57
Figure 4.8	Melting curves associated with decreasing temperature.....	58

1. Introduction

Enterohemorrhagic (EHEC) and enteropathogenic (EPEC) strains of *Escherichia coli* have been associated with hemorrhagic colitis (Jay, 2000) and severe gastrointestinal illnesses (Akinyemi *et al.*, 1998) in humans, respectively. The challenge for identifying these pathogens is their low abundance in the environment (Buchanan and Doyle, 1997). Many monitoring procedures are time consuming and rely on cultivation in a laboratory. A more reliable method for rapid pathogen detection is using molecular techniques that are simple and quantitative. EHEC serotype O157:H7, a predominant *E. coli* pathogen, produces shiga-like toxins and therefore the identification of the virulence gene shiga-toxin 2b (*stx*) provides good indication of the presence or absence of the pathogen. Additionally, EPEC strains of *E. coli* can be identified by the presence of the virulence gene hemolysin A (*hly*). Alternatively, the adenosine kinase (*adk*) gene encodes an enzyme abundantly expressed in homeostatic processes and can be used to identify the presence of all *E. coli* strains, both pathogenic and non-pathogenic.

Conventional methods for characterization of bacteria include immunosensors (Tokarskyy and Marshall, 2008), polymerase chain reaction (PCR) and cultivation (Brichta-Harhay *et al.*, 2007). A practical alternative is the use of biosensors based on nucleic acid hybridizations. Specifically, rapid detection of *E. coli* using impedimetric measurements reduces cost and time required for analyses. Sharp Laboratories of America (SLA) developed an impedimetric platform capable of performing real-time DNA-DNA binding assays. Impedance is the measure of electrical opposition to an applied force. In the SLA platform, an electrical current is applied across electrodes at a fixed frequency, and an integrated reader measures the change in surface impedance. SLA sensor array assays have accurately detected virulence gene markers of *E. coli* from PCR-amplified DNA (Ghindilis *et al.*, 2009; Ghindilis *et al.*, 2010; Ghindilis *et al.*, 2011). Impedimetric detection is able to distinguish between single-stranded (ss)

and double-stranded (ds) DNA based on the difference in their physicochemical properties. Specifically, the negatively charged phosphate backbone of nucleic acids impedes the applied current. Therefore, impedance is sensitive to oligonucleotide concentration and single base pair mismatches (Lisdat and Schafer, 2008), allowing for very specific detection of nucleic acids.

There have been several editions of the SLA platform. Version IA-1 included eight gold interdigitated microelectrodes (GIMEs) that were functionalized with DNA oligonucleotide probes bound to the surface through sulfhydryl chemistry (thiolate formation) (Leung *et al.*, 2008). The GIME surface was contained in a chamber with two cells of 25 μ l volume each enclosing four electrodes, which enabled two independent assays (Ghindilis *et al.*, 2009, Ghindilis *et al.*, 2010 and Messing *et al.*, 2010). The IA-2 platform included a new reader instrument that was able to perform simultaneous, real-time measurements of multiple electrodes. The GIME surface contained 15 microelectrodes enclosed within a three cell chamber (5 microelectrodes per chamber), and the system had an integrated software package for real-time analysis (Ghindilis *et al.*, 2012). The current IA-3 platform is smaller and allows for a higher applied frequency and impedance load (10-10000 Hz and 1000 M Ohms, respectively).

A wide spectrum of bacterial species and strains can be targeted by DNA-DNA hybridization. Gene probes are frequently used for immunological applications in the food industry and industrial water supplies to monitor contaminating organisms (Rodriguez-Mozaz *et al.*, 2004), and are starting to play an important role in environmental monitoring.

The Center for Coastal Margin Observation and Prediction (CMOP) is an NSF Science and Technology Center (STC) that provides an interdisciplinary approach to understanding the coastal margin ecosystem. In collaboration with SLA, CMOP investigators are developing real-time analyses for rapid detection of microorganisms in river, estuarine and coastal waters. A

major focus for CMOP is the Columbia River, which has the second largest freshwater drainage basin in the United States (USGS fact sheet, 2013). The Willamette River, a major tributary to the Columbia River, receives pollution input from a variety of sources including wastewater treatment plants, industrial sewage and urban and agricultural runoff (Oregon DEQ, 2012). These point and non-point sources of pollution can introduce harmful bacteria to natural ecosystems. This is increasingly important because both the Columbia and Willamette rivers harbor native and endangered salmonids (Altman *et al.*, 1997) and are in frequent use for recreational and industrial purposes. Thus, the level of pollution in the river is a major concern for economic stability and human health.

Water systems in close proximity to urbanized land have extensive pollution input and therefore contain elevated levels of enteric bacteria, including *E. coli*, in comparison to rural lands (Belt *et al.*, 2007). Urbanized coastal waters are correlated with higher abundances of fecal coliform bacteria, including pathogenic strains, which lead to water-borne illnesses (Mallin *et al.*, 1999). The ecological implications of contaminated water systems are the destruction of habitats and risk of infectious disease in humans (Chen *et al.*, 2004). Water quality can be improved by finding the source of the contamination. In the Tillamook basin (OR), for example, the presence of fecal bacteria was linked to ruminant and human sources, but it was difficult to determine the origin of the contamination in the water (Shanks *et al.*, 2006). *E. coli* is often used as a fecal indicating bacterium (FIB) for identifying the presence of water-borne pathogens due to its association with fecal coliform bacteria (Meays *et al.*, 2004). FIB monitoring can aid in identifying the origin of pollution in water systems, but often misdiagnoses pathogen risk in the environment because it does not accurately measure the virulence of the identified *E. coli* in a

sample. Rapid characterization of virulence gene markers from *E. coli* using the SLA detection method could enhance the specificity of environmental monitoring practices.

Scientists at the Monterey Bay Aquarium Research Institute (MBARI) developed the environmental sample processor (ESP), a novel platform used to target organisms by performing sandwich hybridization array (SHA) assays. The ESP is autonomous and performs *in situ*, subsurface molecular diagnostic tests remotely (Scholin, 2009). The ESP core system can directly target species by a procedure of sample collection, sample processing to produce cell lysate and performing SHA assays based on 16S rRNA gene targets. In addition, the ESP has a sample archive function (preserved whole cells) for later testing in the laboratory (Doucette *et al.*, 2009; Greenfield *et al.*, 2006; Scholin, 2009). The ESP is a reliable instrument for molecular biological analyses in the field, however, the ESP detection technology is expensive and the chemiluminescence data from the SHA assays only provides qualitative information on the presence/absence of a targeted organism. Integration of the SLA sensor array would provide an impedance-based DNA hybridization assay in an inexpensive, label-free and re-useable format. The SLA sensor array can detect target marker genes, thus in conjunction with the ESP would facilitate near real-time monitoring of pathogens in the environment. In addition, the ESP can adaptively sample by triggering sampling events based on changes in environmental parameters. Linking pathogen abundance to environmental variables, such as changes in temperature and salinity, may provide a better understanding of factors that influence the virulence of pathogenic populations.

The main goals of this thesis were to develop and test new SLA formats and optimize hybridization assays for discrimination of different *E. coli* strains, both pathogenic and non-

pathogenic. Broadly, research in this thesis aided the development of a field-based biosensor for rapid, high-resolution monitoring of the environment. The major questions addressed were:

- Can the SLA impedimetric platform perform hybridization assays for full-length gene-based targets?
- Is the impedance signal response for specific targets enhanced by use of multiple probes?
- How does hybridization with different target types affect assay signal response?
- Is the SLA platform a good candidate for use as a universal detection system for pathogenic organisms in the environment?

In addition to this introduction and a final conclusion chapter, this thesis is organized into three data chapters that focus on the questions above. Chapter 2 addresses the detection of full-length dsDNA targets using the SLA impedimetric platform and improving assay response by optimizing hybridization parameters. Chapter 3 discusses the potential application of the SLA platform as a universal detection system and describes the detection of full-length ssDNA targets. Finally, Chapter 4 investigates the improvement of assay specificity by use of sensor arrays functionalized with multiple probes and analysis of melting curves.

2. Genomic DNA-based Assay Development

2.1 Introduction

2.1.1 Environmental monitoring

Natural water sources contaminated with waste can harbor pathogens that are a health risk to humans and the environment. Pathogen contamination often comes from storm water flooding and sewage spilling which introduces fecal matter and associated microorganisms into the water. There is a direct relationship between an increase in fecal contamination in freshwater systems and an increase in detectable enteric bacteria (Ishii and Sadowsky, 2008). Several nucleic acid hybridization assays are available for detection and characterization of bacterial species in environmental samples. Development of novel, label-free biosensors that employ impedimetric detection are useful because they allow for rapid detection in real-time. Other technologies that require labeling of an analyte rely on end-point reactions and the amount of label detected corresponds to the number of bound analytes. Real-time detection is limited in these methods and quantification is highly variable (Wagner *et al.*, 2007). In contrast, impedance-based detection methods are inexpensive, methodologically simple and allow for simultaneous data analysis (Daniels and Pourmand 2007).

2.1.2 Impedimetric biosensors

There are a number of impedance-based sensors that are able to detect antibody-antigen interactions (Barreiros dos Santos *et al.*, 2009 and Mejri *et al.*, 2010) and DNA hybridization events (Liu *et al.*, 2009 and Zhang *et al.*, 2009). Most of these sensors measure an impedance signal at varying frequencies. A more effective approach is to measure impedance at a fixed frequency, which reduces time required for each measurement and provides a more accurate measure of the output signal. SLA has developed instrumentation capable of measuring

impedance of multiple electrodes simultaneously at a fixed frequency, while an integrated algorithm enables quantification of real-time data (Ghindilis *et al.*, 2010 and Messing *et al.*, 2010). Because the sensor arrays have a gold surface, detection of different target types (e.g., antibodies and nucleic acids) is simple and robust through functionalization with sulfhydryl chemistry. Functionalization immobilizes a thiol-modified DNA probe to an array surface prior to introduction of the analyte. When an analyte is specific to the DNA probe, the electrical properties (i.e., impedance) of the array surface change as a result of the interaction between the probe and target (Skladal, P. 1997; **Figure 2.1A**).

2.1.3 DNA-based detection

Previous studies using the SLA platform demonstrated the detection of short (20-35 nucleotide [nt]), cDNA targets (Ghindilis *et al.*, 2009) and longer (193-355 base pairs [bp]), PCR-amplified DNA targets (Ghindilis *et al.*, 2010 and Messing *et al.*, 2010). In these studies, nucleic acid assays distinguished three gene targets from closely related *E. coli* strains. The gene targets were distinguishable because immobilized DNA probes hybridized to the complementary target alone. The other two non-complementary analytes remained unbound and therefore did not significantly alter array surface properties. The impedance response signal was significant for a specific target at a low detection limit of 5-10 nM. These studies displayed an impedance biosensor that successfully detects a variety of analytes and is practical in a laboratory setting. A major challenge of DNA-based assays is cross-hybridization of the non-complementary targets. Thus, reducing non-specific interactions is an important consideration in the development of a reliable detection method. A dependable impedimetric platform has potential for further integration with an amplification module, which is amenable for field monitoring. Effective environmental monitoring also requires the capability to detect full-length gene targets in mixed

consortia. Therefore, more studies are needed that focus on the detection of targets similar in size to targets isolated from environmental samples and present among a variety of non-specific targets.

2.1.4 Aims of this study

This chapter describes in detail the work published in Ghindilis *et al.*, 2012. The main goal of this study was to develop a full-length, PCR-amplified dsDNA assay for microbial detection using the SLA impedance biosensor. The SLA platform allows for swift analysis of DNA-DNA binding kinetics. Streamlining sample processing is important for rapid monitoring of the environment because after cell lysis, intact genetic materials degrade relatively rapidly. As such, dsDNA targets were chosen over ssDNA targets because using them reduces sample preparation steps. Three gene targets were used for detection of *E. coli*, including pathogenic strains. A major aspect of assay development was eliminating binding events that diminish the specific target:probe signal. These events included renaturation of dsDNA and non-specific binding to probes. Therefore, we illustrated that optimizing assay parameters helped to reduce unwanted binding, thereby providing good separation between specific and non-specific binding responses. My thesis research involved the DNA target preparation, performance of hybridization assays and data analysis.

2.2 Materials and Methods

2.2.1 Sensor arrays

Sensor arrays were developed and manufactured at SLA. Each sensor array contained (1) a gold surface that allowed for different biochemical and chemical functionalization schemes; (2) a reader that takes measurements from multiple electrodes in real-time; and (3) an integrated

software package for rapid quantification and analysis of data. There are several generations of the platform (described in Chapter 1); this study utilized the IA-2 platform.

2.2.2 Array fabrication and functionalization

Each sensor array contained 15 gold electrode pairs (with 40-micron gaps) on glass, fitted with a fluidics chamber consisting of three independent cells enclosing five electrode pairs (**Figure 2.1B**). Sensor arrays were functionalized by SLA using oligonucleotide probes (Integrated DNA Technologies [Skokie, IL]) that were thiol-modified on the 5' end for surface attachment (Ghindilis, *et al.*, 2009). The following 20 nt probes ($T_m = 55^\circ\text{C}$) were designed from *E. coli* target amplicons: (1) p-*adk*, 5'-TGGAGAAATATGGTATTCCG-3', (2) p-*hly*, 5'-TGAATTCCAGAAGCAAGTCT-3', and (3) p-*stx*, 5'-GCGGTTTTATTTGCATTAGT-3' (**Table 2.1**). Array functionalization QC tests done with fluorescent microscopy are described in Ghindilis *et al.*, 2010 and Messing *et al.*, 2010.

2.2.3 Instrumentation

The IA-2 instrument is capable of measuring up to 15 channels simultaneously, with eight impedance measurements per second per channel, at a fixed stimulation frequency and voltage (ranges of 10-1000 Hz and 10-212 mV, respectively). The instrument is also equipped with temperature control at the sensor surface.

2.2.4 DNA target preparation

Three dsDNA targets were prepared by PCR from genomic DNA of three *E. coli* strains. The *adk* amplicon, a 193 bp fragment of the adenylate kinase gene, was amplified using the primers *adk*-F, 5'-ATTCTGCTTGGCGCTCCGGG-3, and *adk*-R, 5'-CCAGCGCGATCACCAGTTCG-3 (Wirth *et al.*, 2006) from the commensal *E. coli* K-12 isolate MG1655 (Blattner *et al.*, 1997), and the uropathogenic isolate *E. coli* CFT073 (Welch *et al.*,

2002). Two other targets were selected from gene markers of EPEC and EHEC *E. coli* strains. The *hly* amplicon, a 355 bp fragment of the alpha-hemolysin gene, was amplified using the primers hly-F16, 5-CAGTCCTCATTACCCAGCAAC-3, and hly-B14, 5-ACAGACCCCTTGTCCTGAAC-3 from the EHEC strain EDL 933 (O157:H7) (Perna et al., 2001), and CFT073. Finally, the *stx* amplicon, a 269 bp fragment of the Shiga toxin 2b gene, was amplified using the primers stx-GK5, 5-ATGAAGAAGATGTTTATG-3, and stx-GK6, 5-TCAGTCATTATTAAGT-3 (Beutin et al., 2009) from the EDL 933 strain.

PCR mastermix was made in 1 ml volumes containing the following reagents: 500 µl iQ 10X supermix (Bio-Rad, USA), 500 µl water, 20 µl 1 µM forward primer, 20 µl 1 µM reverse primer and 2 µl template (genomic DNA). PCR conditions were as follows:

Denaturation at 94°C for 2 min, followed by 40 cycles of (1) denaturing at 94°C for 30 sec, (2) annealing at 60°C for 30 sec (50°C for *stx*), and (3) extension at 72°C for 1 min. Finishing with final extension at 72°C for 7 min.

PCR amplicons were analyzed by gel electrophoresis on 1% agarose gel containing 1 µg·ml⁻¹ of GelRed (Biotium). The amplicons were purified using QIAquick PCR Purification Kit (Qiagen, Valencia, CA), and DNA concentrations were analyzed using a NanoDrop spectrophotometer (Thermo Scientific, Wilmington, DE). PCR primers and amplicons are shown in **Tables 2.2** and **2.3**, respectively.

2.2.5 Sensor array assays

Assays targeting the *adk*, *hly* and *stx* genes were done on sensor arrays functionalized with p-*adk*, p-*hly* and p-*stx*, respectively. Assays were performed in hybridization buffer (2x SSPE containing 20 mM Na₂EDTA and 0.05% Tween-20 [0.3 M sodium chloride, 0.02 M sodium phosphate and 1 mM Na₂EDTA]). The dsDNA targets were denatured at 95°C for 5 min

prior to immediate injection into sensor array chambers. Impedimetric measurements were performed at 24 Hz and 100 mV, and the current:voltage ratio provided a Z value of surface impedance, measured in Ohms. Target-free buffer was injected into chambers to establish a baseline, after which the buffer containing either complementary or non-complementary (control) dsDNA targets was injected.

2.2.6 Data analysis program

Data analysis software integrated in the IA-2 platform (**Figure 2.1B**) consisted of a mathematical algorithm (Ghindilis *et al.*, 2010; Messing *et al.*, 2010) used to extract DNA-DNA binding kinetic parameters from the impedance signal. Hybridization of complementary targets to the array resulted in a binding curve, measured over time. The impedimetric binding curve is represented by Eq. (1):

$$Z(t) = B - Ae^{-st}$$

where B , A and s are independent constants. B is the offset of the exponential curve and is representative of the baseline impedance signal. A is the amplitude of the resulting impedance signal, and s is the exponential time constant. The data algorithm automatically calculates constants A and s and averages the signal of the five electrodes for each chamber. Integrated area is an additional parameter from the impedance signal response and is calculated as the area under the binding curve 600 sec post-injection.

2.2.7 Assay optimization

Sensor array assays were optimized with dsDNA targets to achieve maximum impedimetric response for a specific target and minimum response for a non-specific target.

Initially, assay parameters examined were target concentration (0.5 and 2.5 $\mu\text{g}\cdot\text{ml}^{-1}$), buffer concentration (1x, 2x and 4x SSPE), voltage (40, 75, 100 and 150 mV) and temperature (47 and 52 °C). All assays were performed at 75 Hz on arrays functionalized with p-*adk*, with *stx* and *hly* dsDNA targets used as negative controls. For each experiment, all three target amplicons were used for injections into three reaction chambers on the same sensor array. Additional testing of target concentrations in the range of 1-1000 $\text{ng}\cdot\text{ml}^{-1}$ was done by scientists at SLA.

Assays using sensor arrays functionalized with p-*stx* were optimized to improve specific detection of the *stx* target with *adk* and *hly* dsDNA targets serving as negative controls. Initially, assays were performed with the parameter settings of the optimized *adk* assay, then, assay parameters tested were target concentration (5, 50 and 500 $\text{ng}\cdot\text{ml}^{-1}$), buffer detergent (0.05% Tween-20 or 0.1% Triton X100) and temperature (30, 40 and 50 °C). Assays were performed at 75 Hz and 75 mV in 2xSSPE buffer.

The *hly* assay was optimized on sensor arrays functionalized with p-*hly*. Initial assays were performed with the optimized *stx* assay parameters after which buffer concentrations of 1x, 2x and 6x SSPE were tested. Hybridization assays were performed at 75 Hz, 75 mV, target concentration of 10 $\text{ng}\cdot\text{ml}^{-1}$ and temperature of 30°C.

2.3 Results and Discussion

2.3.1. Gene-based detection of dsDNA targets

Hybridization assays were executed on sensor arrays functionalized with p-*adk* for specific detection of the *adk* dsDNA target. Prior to injection, dsDNA targets were denatured at 95°C for 5 min to separate sense and anti-sense strands and facilitate binding of the sense strand to the complementary probe on the sensor surface. In each experiment, after obtaining a baseline with buffer injection, one chamber was injected with a target complementary to the probe and the

other two chambers were injected with non-complementary controls. Binding curve response parameters for *adk* were not significantly different compared to negative controls (data not shown). Unlike previous work with short ssDNA in which specific and non-specific impedimetric responses were easily distinguishable (Ghindilis *et al.*, 2009), preliminary results with full-length dsDNA targets exposed an additional challenge. Injecting both sense and anti-sense strands into chambers introduced competitive interactions that can inhibit impedimetric signal of sense target:probe hybridization. In addition to the sense strand binding, the following events could also occur: (1) renaturation of the original dsDNA strands, (2) non-specific binding of the anti-sense strand with the probe, (3) cross-hybridization of the negative controls and (4) non-specific binding of the probe to an unintended region of the sense strand. These processes compete for limited access to probes, thereby dampening the response curve and underlining the need for extensive assay optimization.

2.3.2 Assay optimization

Each gene-specific hybridization assay was optimized by testing a range of one assay parameter at a time and selecting which value of that parameter gave the best separation of the specific and negative control target responses. Assays performed on p-*adk* functionalized sensor arrays were initially optimized with the following parameters: target concentration of 0.5 $\mu\text{g}\cdot\text{ml}^{-1}$, buffer (SSPE) concentration of 2x, voltage of 75 mV and temperature of 52°C. Further optimization of target concentration was performed to determine the assay detection limit. Results revealed a significant difference in impedance signal for the specific (*adk*) target compared to the non-specific (*hly* and *stx*) targets (**Figure 2.2A**). The amplitude *A*, integrated area and *A*s* values were four orders of magnitude higher for *adk* than negative controls (**Figure 2.2B**). These data indicated the *adk* assay detected the *adk* gene target in a specific manner,

allowing for distinction of different *E. coli* strains. The *adk:stx* and *adk:hly* ratios of amplitude *A* and integrated area show clear optima at a target concentration of 100 ng·ml⁻¹. Alternatively, the time constant *s* ratios showed no clear optimum across target concentrations (**Figure 2.3**). Time constant *s* ratios were higher at the higher target concentration which may be a result of the target:probe binding reaching saturation at higher target concentrations. Thus, optimization of target concentration obtained a good separation of specific and non-specific impedance responses for two of the three binding curve parameters.

Assays performed on arrays functionalized with p-*stx* were optimized. Binding curves were analyzed for *stx:adk* and *stx:hly* ratios and their dependence on differing assay parameters. Amplitude *A* showed a 10x lower optimum for target concentration than the *adk* assay (10 ng·ml⁻¹ versus 100 ng·ml⁻¹). Additionally, hybridization buffer detergent was optimized using 0.1% Triton X100 over the use of 0.05% Tween-20 (data not shown). An assay temperature of 30°C increased the specificity of target binding for amplitude *A*, but time constant *s* showed weak target binding at this temperature. Conversely, at 50°C, time constant *s* showed a greater difference between specific and non-specific hybridization, while the amplitude yielded lower separation of the specific target and negative control signals (**Figure 2.4**). This finding displayed the need for an additional binding curve analysis parameter, the initial binding rate *A*s*, to distinguish differences in the binding curve between specific and non-specific hybridizations.

DNA targets *stx* and *adk* serve as good controls for one another because they share no sequence similarity. Conversely, *hly* and *adk* are partial-complementary, resulting in cross-hybridization. To mitigate this effect, we examined the effect of ionic strength on the efficiency of DNA binding by optimizing the hybridization buffer concentration. Binding curve parameters

were analyzed for assays performed on p-*hly* functionalized arrays. Amplitude A exhibited the highest *hly:stx* and *hly:adk* ratios with a buffer concentration of 1x SSPE (**Figure 2.5**).

Each gene-based assay showed different optimization needs (**Table 2.4**), suggesting that hybridization kinetics are sequence-dependent. Assays were extensively optimized, however, all possible combinations of parameters were not tested due to time constraints. We successfully illustrated that the SLA impedimetric platform is able to specifically detect and differentiate strains of *E. coli* in real-time. Additionally, optimization played an important role in assay development to achieve the maximum specific signal response in comparison to non-specific signal response.

Table 2.1. Probes (20 nt) designed to target different *E. coli* strains.

Probe	Probe sequence	Target strain (<i>E. coli</i>)
adk-1	5'-TGG-AGA-AAT-ATG-GTA-TTC-CG-3'	All strains
adk-2	5'-AGG-GAC-TCA-GGC-TCA-GTT-CA-3'	
hlyA-1	5'-TGA-ATT-CCA-GAA-GCA-AGT-CT-3'	(EHEC) EDL933, CFT073
hlyA-2	5'-GGC-AGT-CCG-GAA-AAT-ATG-AA-3'	
stx2b-1	5'-GCG-GTT-TTA-TTT-GCA-TTA-GT-3'	(EHEC) EDL933
stx2b-2	5'-GGA-TTG-CGC-TAA-AGG-TAA-AA-3'	

Table 2.2. Forward and reverse primer sequences used for full-length PCR amplification of *E. coli* genes.

Gene	Primer	Primer sequence	Amplicon Length (bp)
<i>adk</i>	adk-F	5'-ATT-CTG-CTT-GGC-GCT-CCG-GG-3'	193
	adk-R	5'-CCA-GCG-CGA-TCA-CCA-GTT-CG-3'	
<i>hlyA</i>	hlyA-F16	5'-CAG-TCC-TCA-TTA-CCC-AGC-AAC-3'	355
	hlyA-B14	5'-ACA-GAC-CCC-TTG-TCC-TGA-AC-3'	
<i>stx2b</i>	GK5	5'-ATG-AAG-AAG-ATG-TTT-ATG-3'	269
	GK6	5'-TCA-GTC-ATT-ATT-AAA-CTG-3'	

Table 2.3. Sequences of *E. coli* genes targeted for hybridization with 20 nt probe sequences.

Target	Target sequence
<i>adk</i>	5'-AGTTCATCATGGAGAAATATGGTATTCCGCAAATCT-3'
<i>hlyA</i>	5'-TGACTATTATGAAGAAGGAAAACGTCTGGAGAAAA-3'
<i>stx2b</i>	5'-CGGATTGCGCTAAAGGTAAAATTGAGTTTTCCAAG-3'

Table 2.4. Optimal conditions for three gene-based assays.

Assay	Parameters			
	[Target] (ng·ml ⁻¹)	[Buffer SSPE]	Voltage (mV)	Temperature (°C)
<i>adk</i>	100	2x	75	52
<i>stx</i>	10	2x*	75	30
<i>hly</i>	10	1x	75	30

*Buffer detergent optimized with 0.1% Triton X100

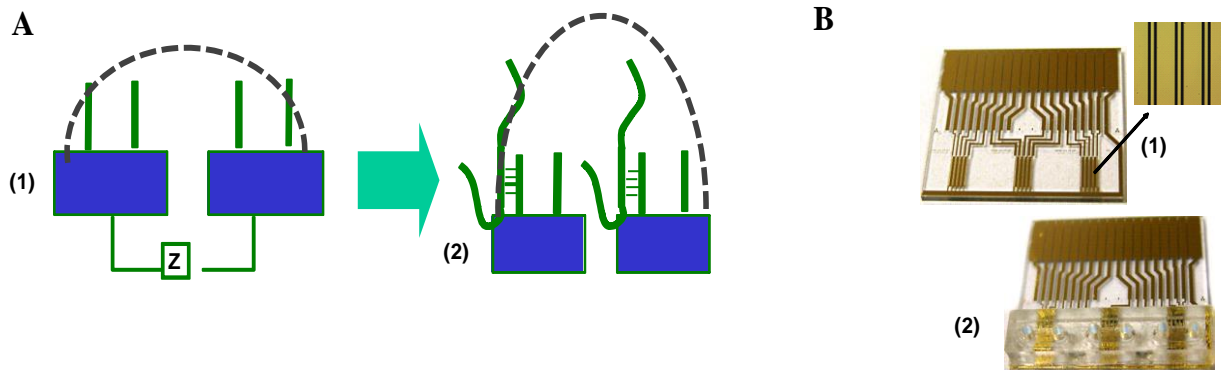


Figure 2.1. SLA impedance sensor array. (A) *Impedimetric (z) detection scheme, (1) functionalized sensor array prior to target injection has baseline signal (dotted line) and (2) target analyte binds to probe on sensor surface and impedimetric signal (dotted line) increases.* (B) *SLA sensor array contains (1) individual gold interdigitated microelectrodes and (2) an attached reaction chamber with three cells.*

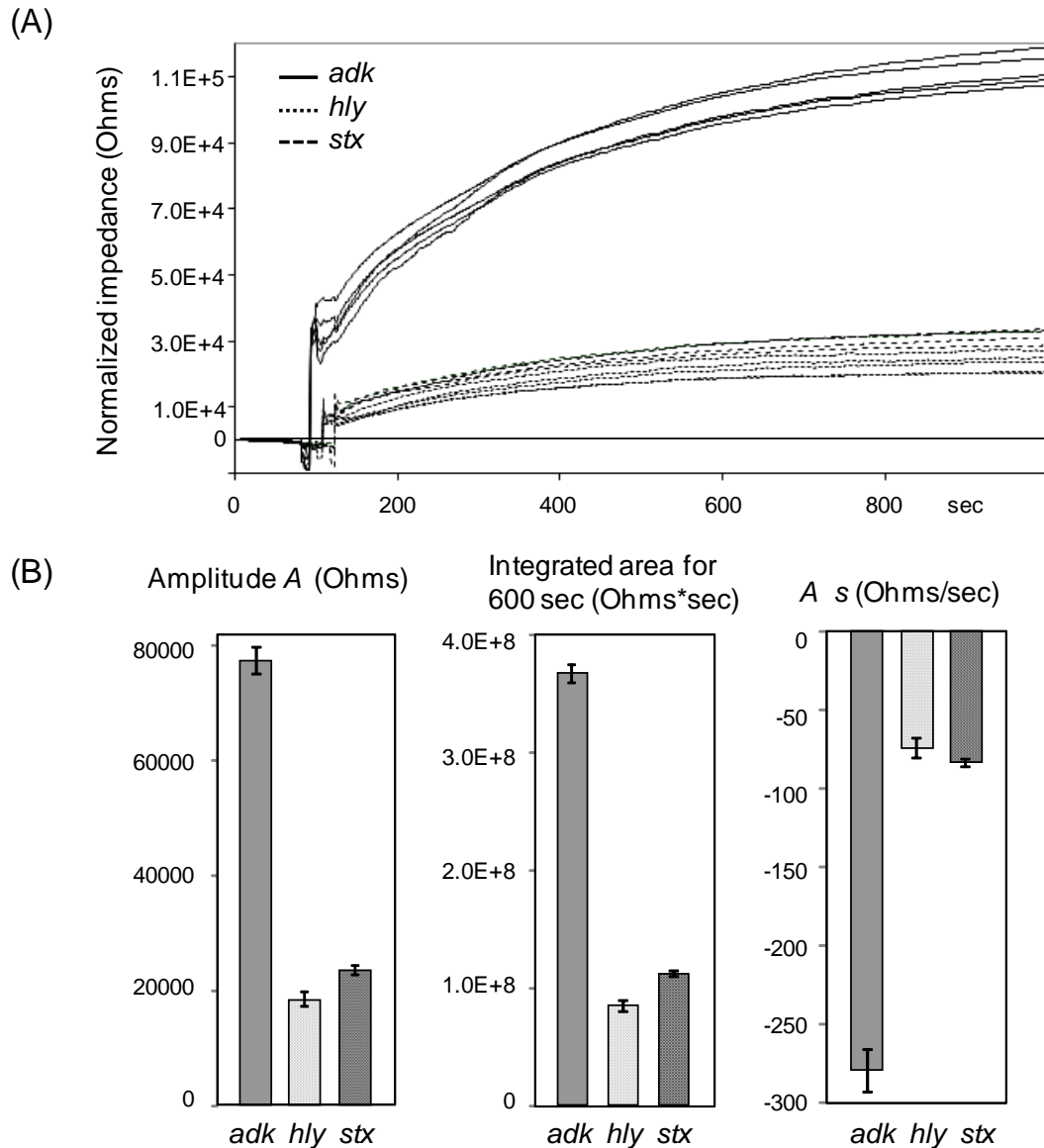


Figure 2.2. Adk assay optimization. (A) Binding curves of the normalized impedance signal obtained for the specific *adk* target amplicon (solid lines), and the non-complementary *hly* and *stx* negative control amplicons (dotted lines). (B) The binding curve parameters calculated for the complementary *adk* targets (grey bars), and the negative controls *hly* and *stx* (dotted and hatched bars, respectively). Each bar is an average calculated from measurements of 5 different microelectrodes within a reaction chamber. Error bars indicate standard deviations.

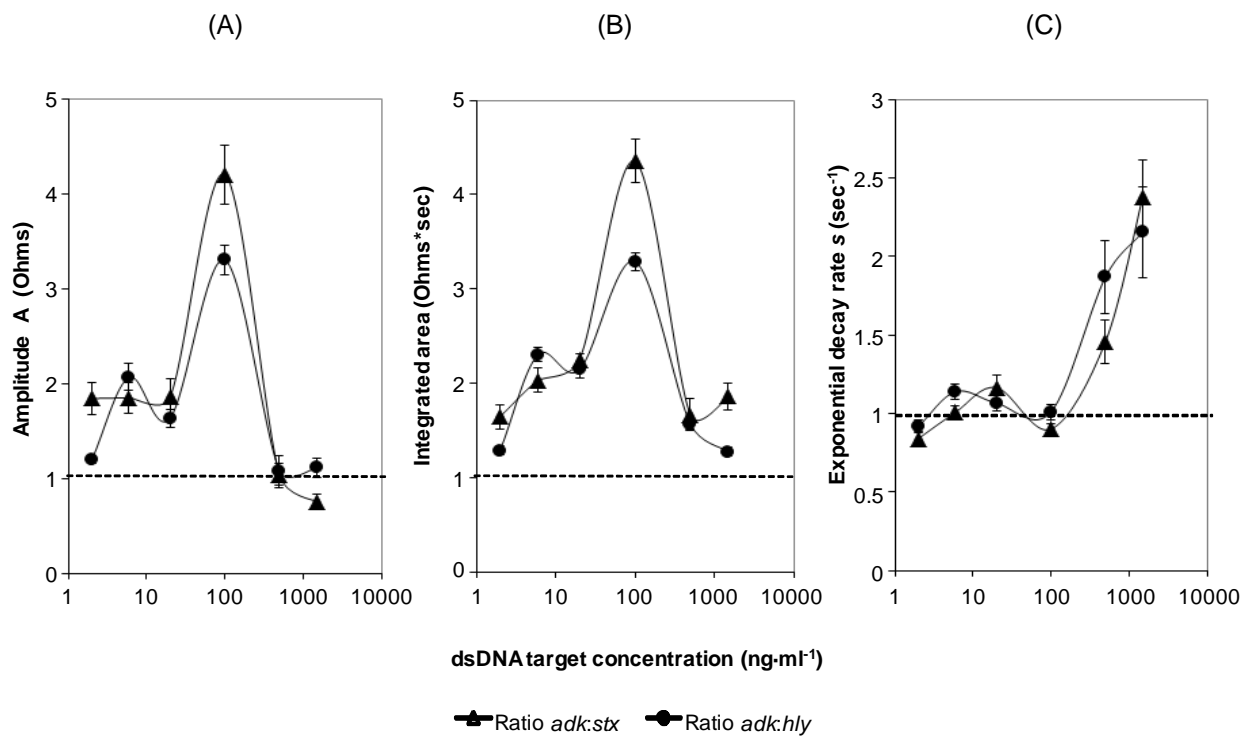


Figure 2.3. Adk detection limit. Ratios (Y-axis) between the impedance response parameters obtained for the specific *adk* versus the negative control (*stx* or *hly*, triangle or circle, respectively) targets at 6 different concentrations (X-axis) were calculated for the following parameters: (A) amplitude A, (B) integrated area calculated for 600 sec and (C) exponential decay rate s . Each parameter value is an average calculated from measurements of 5 different microelectrodes within a reaction chamber. Error bars indicate standard deviations.

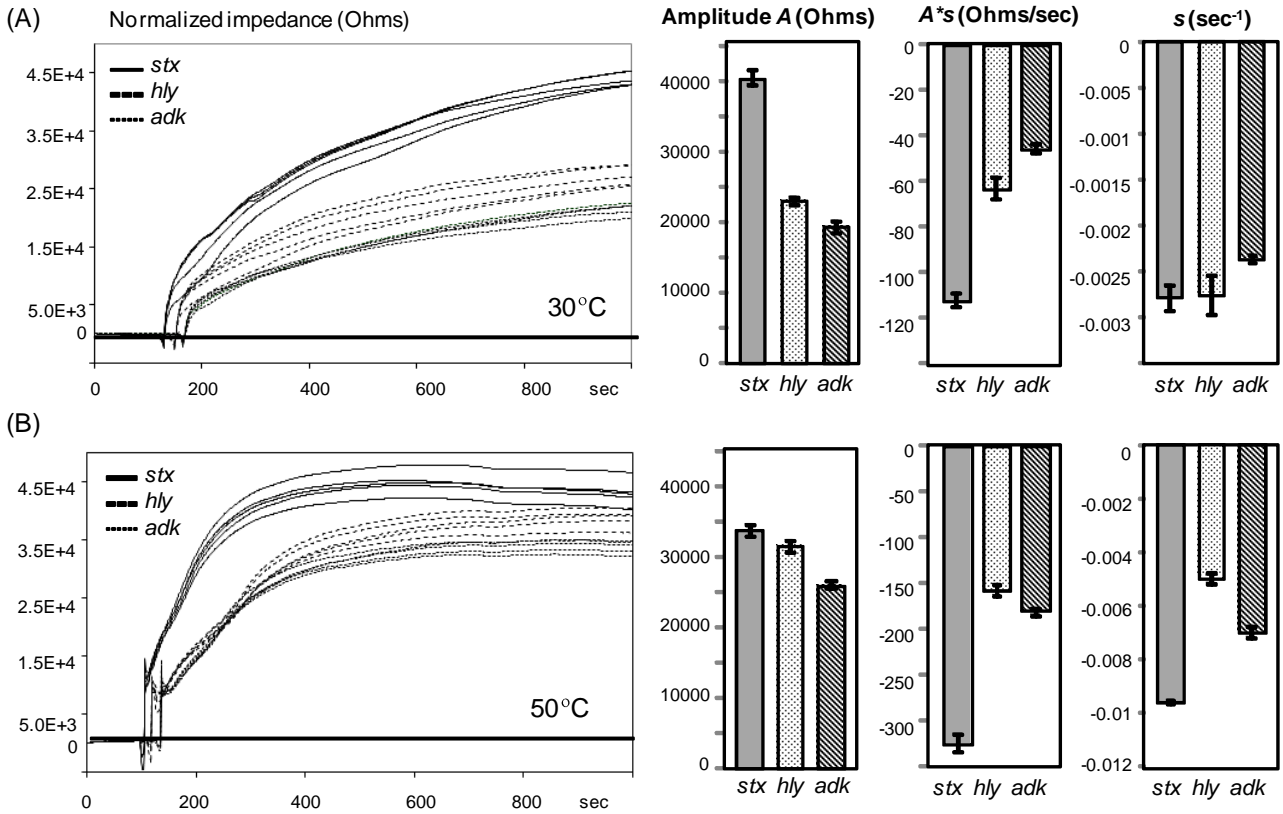


Figure 2.4. Stx assay optimization. Hybridization temperatures analyzed were 30 and 50 °C, for (A) and (B), respectively. Left panels show binding curves of the normalized impedance signal obtained for the specific *adk* target amplicon (solid lines), and the non-complementary *hly* and *stx* negative control amplicons (dotted lines). Right panels show binding curve parameters calculated for the complementary *adk* targets (grey bars), and the negative controls *hly* and *stx* (dotted and hatched bars, respectively). Each bar is an average calculated from measurements of 5 different microelectrodes within a reaction chamber. Error bars indicate standard deviations.

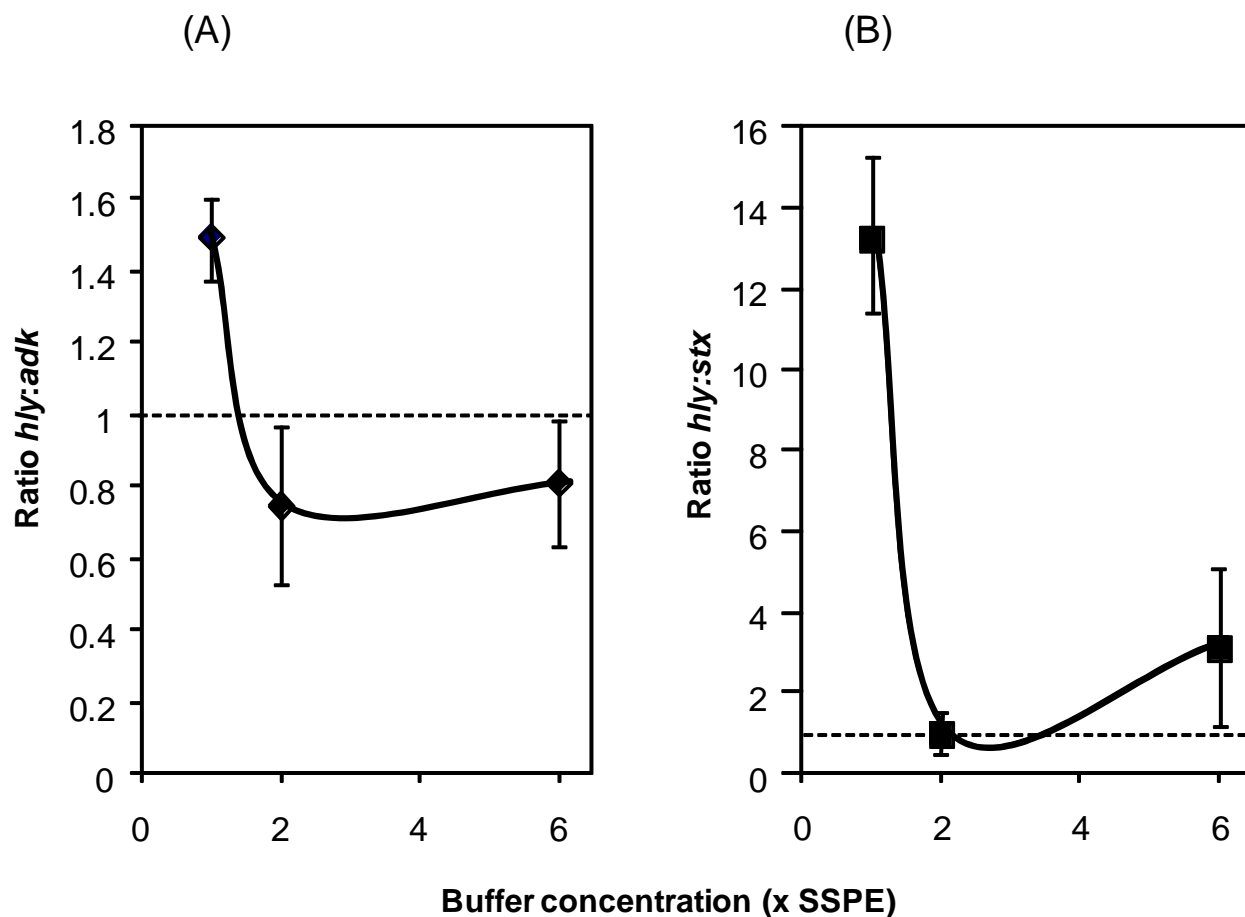


Figure 2.5. *Hly* assay optimization. Ratios (Y-axis) of the impedance response amplitude *A* were calculated for the specific *hly* versus the negative control targets: (A) partially complementary *adk* (diamonds) and (B) non-complementary *stx* (squares) at 3 different SSPE buffer concentrations (X-axis). Each point is an average calculated from measurements of 5 different microelectrodes within a reaction chamber. Error bars indicate standard deviations.

3. Universal sensor array

3.1 Introduction

3.1.1 User-friendly technology

One of our long-term goals is to develop an integrated detection system for environmental monitoring that incorporates sample extraction and purification, DNA amplification by real-time PCR and a bio-sensing technology. Impedimetric biosensor methods are optimal for robust and real-time analyses. Our collaborators at SLA have made substantial progress towards developing and manufacturing an impedimetric platform amenable to field use. One of the major challenges for producing an inexpensive, accessible instrument is mass-producing and supplying sensor arrays to markets with different application interests. In order to develop sensor arrays that have flexible use, SLA pre-functionalized sensor arrays with a polyG oligonucleotide probe that was complementary to polyC-modified gene-specific probes for functionalization with any target of interest (**Figure 3.1**). At CMOP, we are interested in environmental monitoring of pathogenic microorganisms, and immobilizing probes specific for *E. coli* on sensor arrays already pre-functionalized with polyG probes aided in the development of hybridization assays. This method additionally allowed us to select the desired probe density on each sensor array surface, which aided in assay optimization. Therefore, production of pre-functionalized sensor arrays with polyG probes facilitated detection of a wide spectrum of DNA targets and established a user-friendly technology for all applications.

3.1.2 Detection of RNA targets

The detection of DNA in field samples is important for characterizing which microorganisms are present at any given time, while the detection of RNA is critical for understanding when targeted microorganisms are active in the environment (Call *et al.*, 2003). Specifically, a better understanding of when pathogenic microorganisms are both present and

active in the environment is important for human health risk assessment (Huang *et al.*, 2006) and investigating how pathogen abundances are affected by ecosystem variability (Wang *et al.*, 1997). Specific detection of RNA targets enables high-resolution monitoring by providing information on activity, but it also introduces the challenge of processing samples rapidly. Rapid, real-time detection is especially important for RNA because transcripts degrade quickly due to nucleotide cleavage by ubiquitous RNase enzymes in the environment (Hajnsdorf *et al.*, 1994). The first steps toward RNA detection with the SLA platform used full-length single-stranded cDNA (designated ssDNA) gene targets (200-400 bp in length) prepared by reverse transcription. Employing ssDNA is beneficial because it eliminates renaturation associated with dsDNA targets, the full-length targets are representative of standard gene fragments evaluated in environmental surveys, and the ssDNA is similar to rRNA targets, which are also single-stranded. We conjecture that changes to array surface properties are correlated to target biomolecule size, and therefore longer ssDNA strands would increase the impedance signal. Because only 20 bp of a target hybridizes to a probe, we also expect any unbound DNA that remains in the aqueous environment to increase the impedance signal. Transitioning from the detection of ssDNA to RNA targets would require the development of an RNase-free sensor surface environment to reduce RNA degradation rates. Furthermore, DNA probes complementary to the sense strand of the DNA target would be replaced with probes complementary to the anti-sense strand of the RNA target. Lastly, hybridization assays using RNA targets would require optimization to achieve maximum impedance response for specific targets and minimum impedance response for negative controls.

3.1.3 Aims of this study

The main goals of this study were to show an effective pre-functionalization technique with the SLA sensor array and its capability for performing hybridization assays using full-length ssDNA targets. SLA pre-functionalized sensor arrays with a 20 nt polyG probe that hybridized to gene-specific probes modified with a polyC fragment on the 5' end (**Figure 3.1**). Hybridization assays using sensor arrays functionalized with polyC-*adk* probes were performed to identify the *adk E. coli* gene target in a specific manner (*hly* target served as the negative control). Here we also tested the new IA-3 platform and its capability to calculate impedance output from assays run at higher frequency and voltage. Moreover, we demonstrated that optimizing assay frequency and voltage greatly improved the differentiation between specific and non-specific ssDNA target signals. My thesis research involved DNA target preparation, functionalization of sensor arrays, performing hybridization assays and data analysis.

3.2 Materials and Methods

3.2.1 DNA target preparation

Preparation of ssDNA targets for *adk* and *hly* was a three-step process (**Figure 3.2**): (1) dsDNA was generated by PCR, (2) RNA was generated from the dsDNA fragment by *in vitro* transcription, and (3) RNA was converted to ssDNA by reverse transcription. The dsDNA fragments (1) were constructed by PCR (detailed description in Chapter 2.2.4) with *adk*-F and *hly*-F16 primers modified by the addition of a promoter recognized by T7-polymerase; reverse *adk* and *hly* primers were unmodified. After PCR amplicons for *adk* and *hly* (193 and 355 bp, respectively) were purified, the T7-promoter labeled sense strands were used as templates for *in vitro* transcription (IVT) using the MEGAscript Kit (Ambion, USA). After IVT, the resulting RNA (in anti-sense orientation) was treated with TURBO DNase to remove template DNA and purified using the MEGAclean Kit (Ambion, USA). RNA was converted to sense ssDNA with

adk and *hly* gene-specific primers using SuperScript III Reverse Transcriptase and treated with RNase H at 37°C for 20 min to remove the RNA template (Invitrogen, USA). PCR was done to confirm that reverse transcription was successful and ssDNA amplicons were analyzed by gel electrophoresis (**Figure 3.2**).

3.2.2 Array functionalization

Sensor arrays pre-functionalized with polyG probes were used in a quality control (QC) protocol (completed by Carmen Campbell at SLA) to confirm that sensor array pre-functionalization was successful. Out of a batch of 20 pre-functionalized sensor arrays, three were selected randomly for testing. The first sensor array was incubated with 500 nM complementary biotinylated-polyC-*adk* probe. A second array was incubated with 1x phosphate buffered saline with 0.05% TWEEN-20 (PBST), and the third with 500 nM non-complementary biotinylated-polyC-*hly* probe. After 45 min at room temperature, arrays were exposed to 1:1000 diluted buffer containing fluoroSperes NeutrAvidin-labeled microspheres (Invitrogen, USA) for 30 min. After 3 washes with 1x PBST buffer, arrays were visualized under fluorescence microscope at 594 nm wavelength and 20X magnification (**Figure 3.3**).

3.2.3 Sensor array assays and optimization

Sensor arrays pre-functionalized with polyG probes were incubated with 1 μM polyC-*adk* probes for 20 min prior to hybridization assays. After incubation, sensor arrays were washed with 2x SSPE buffer 3 times. Assays were performed in hybridization buffer (2x SSPE containing 1% TWEEN-20), 37°C, and 0.1 $\mu\text{g}\cdot\text{ml}^{-1}$ ssDNA. Target-free buffer was injected into all reaction chambers to establish a baseline, after which specific *adk* ssDNA target was injected into one reaction chamber and non-specific *hly* ssDNA target was injected into the remaining two chambers. After a buffer wash, all chambers were injected with specific target (**Figure 3.4**).

Impedimetric measurements were performed at a frequency and voltage of 480 Hz and 25 mV, respectively.

Hybridization assays were optimized with frequency (480 Hz, 4 and 8 KHz were tested) and voltage (25, 100 and 200 mV were tested). All other assay conditions remained the same as above. Binding curve parameters amplitude A , initial binding rate $A*s$ and time constant s were calculated.

3.3 Results and Discussion

3.3.1 Gene-based detection using ssDNA

Hybridization assays were performed on sensor arrays functionalized with polyC-*adk* for specific detection of the *adk* ssDNA target. Prior to injection of targets, buffer was injected into all chambers to obtain a baseline signal. One chamber received two injections of the *adk* target and the other two chambers were injected with the *hly* target followed by the *adk* target. Binding curve response parameters A and s for the *adk* target were not significantly different compared to the negative control. In addition, amplitude A was higher in all three chambers after the second injection of the specific target compared to the first injections of specific target and negative control. A similar amplitude response in all three chambers may be a result of: (1) the negative control cross-hybridizing at a comparable extent as the specific target and (2) inconsistent probe density between chambers, resulting in a low amount of specific target binding after the first injection. Only the initial binding rate $A*s$ revealed a significant difference between the sensor response signals for specific and non-specific targets. Thus, differentiation between specific target and negative control was seen in only one out of three assay parameters (**Figure 3.5**). Additionally, hybridization results showed high variability between different sensor arrays and individual chambers on a single sensor array (data not shown).

We hypothesized that the binding curve parameter values would remain constant in the chamber that received injections of the *adk* target only and that the chambers sequentially injected with the *hly* target and *adk* target would display a significant increase in signal for the specific target injection (**Figure 3.6**). However, this “ideal” response could be obscured for two reasons: (1) the second injection may not show as high of a value for time constant s as the first injection, or (2) only one parameter (A or s) demonstrates a feature close to the ideal response (**Figure 3.7**). Reason 1 could be due to saturation of the probes with bound target or control molecules. Reason 2 could be a result of variability in probe density between chambers on the sensor array surface. Preferably, parameter A would show a higher value than s because it is correlated to high values of integrated area. This would permit an additional separation of specific from non-specific binding, even if s values were the same for both specific and non-specific binding. If parameter s is higher for specific binding, but A is not, the separation between specific and non-specific binding is limited to only one binding parameter. We evaluated our results for their similarity to the idealized response and found that binding curve parameter $A*s$ were similar to an ideal response. However, parameters A and s lacked separation for specific and non-specific target injections, which indicated the need for assay optimization.

3.3.2 Assay optimization

Assays performed on sensor arrays functionalized with polyC-*adk* were optimized using the parameters frequency (8 KHz) and voltage (200 mV). Initially, results revealed that increasing frequency to 8 KHz improved impedance signal for metric amplitude A alone (**Figure 3.8**). Assays further optimized with voltage produced binding curve values for parameters A and $A*s$ that were significantly higher for specific targets compared to non-specific targets; whereas s did not differentiate impedance responses between specific and non-specific targets (**Figure 3.9**).

In addition, impedance signals appeared to double in magnitude for the specific target compared to the non-specific target. Therefore, optimization of assay frequency and voltage obtained clear distinction between specific and non-specific target responses for two out of the three binding curve parameters. We hypothesized that increasing the fixed frequency at which electrodes are stimulated, would diminish the total impedance output and that non-specific target binding would yield an impedance value far below the detection limit. As a result, higher frequency would change the total impedance output by eliminating the measurement of unwanted binding events. Thus, only the binding events that improved impedimetric signal (i.e., specific target binding) contributed to the total impedance signal.

These data indicated that the optimized *adk* hybridization assay detected the *adk* ssDNA target in a specific manner. Additionally, we provided proof of concept for the polyG pre-functionalization technique. Optimization of frequency and voltage improved the assay signal, however, optimal assay conditions were not obtained due to the time requirement for extensive optimization. Additionally, the results still showed high variability between sensor arrays and individual chambers on a single sensor array. QC tests also measured the hybridization of probe:target by comparing the intensity of fluorescence between specific targets and negative controls. These data showed a significant difference between specific and non-specific target responses and the extent of specific target binding was clearer in the fluorescence data compared to the impedimetric assays (data not shown). A higher fluorescence signal could be due to additional wash steps (3X) within the fluorescence protocol. Therefore, post-manufacturing cleaning of sensor arrays could improve impedimetric assay specificity and reliability. Further, QC tests and sensor array assays applied two different measurements for DNA-DNA hybridization and correlating these measurements would potentially reduce the variability issues.

Finally, we successfully illustrated that the SLA impedimetric platform specifically detected full-length ssDNA targets, indicating the possibility of detecting full-length RNA targets in the future.

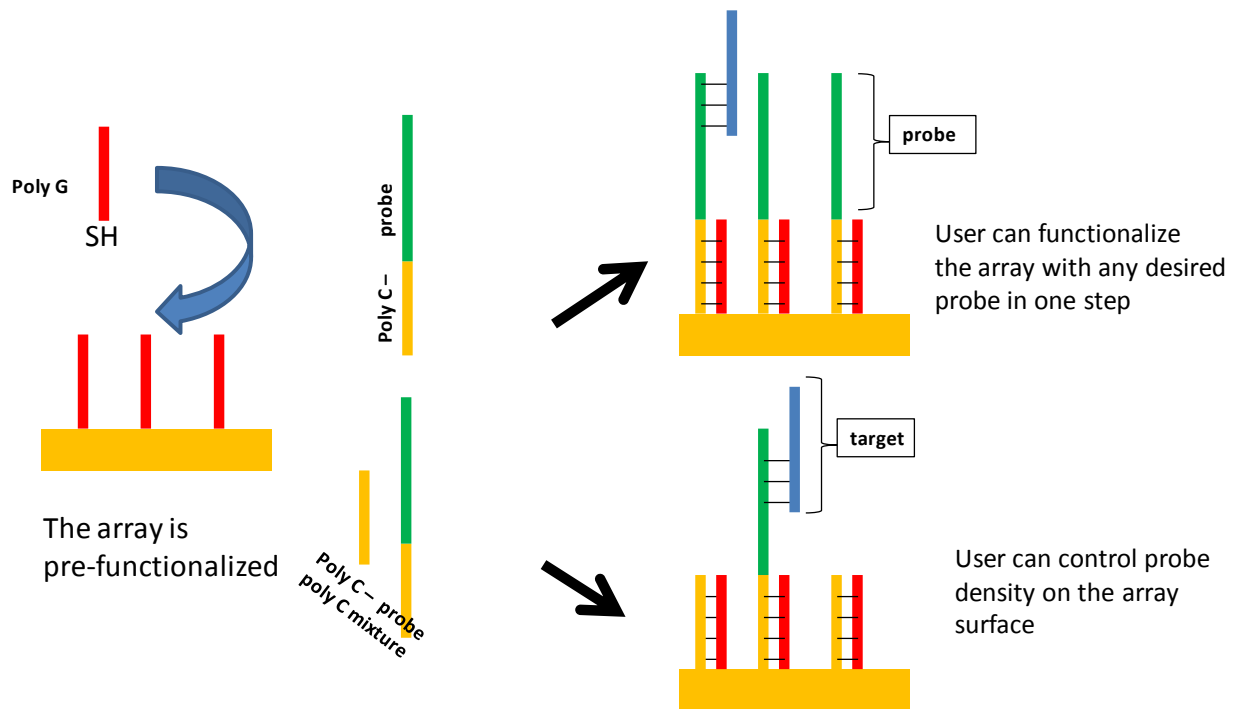


Figure 3.1. Assay functionalization. Left panel indicates pre-functionalization with polyG probes (red lines) followed by functionalization with either polyC-gene-specific probe (green/yellow lines; top arrow) or mixture of polyC-gene-specific and polyC (yellow lines; bottom arrow) probes. Right panel indicates hybridization of polyC-target and specific target (blue lines)

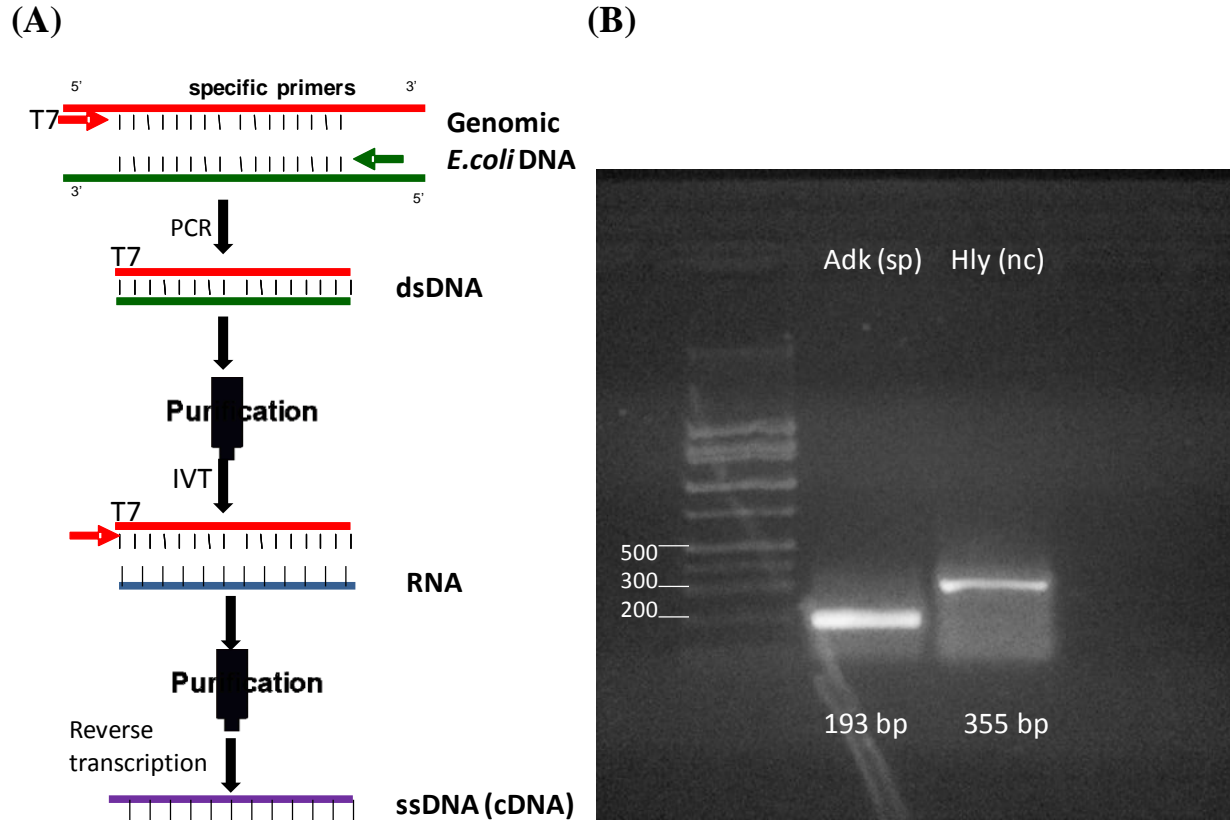


Figure 3.2. ssDNA target preparation. (A) Illustrates the steps for ssDNA preparation: (1) generation of dsDNA (red and green lines) by PCR, (2) generation of RNA (blue line) by in vitro transcription and (3) generation of ssDNA (purple line) by reverse transcription. (B) Shows agarose gel image of PCR-amplified specific (sp) *adk* and negative control (nc) *hly* ssDNA targets at 193 and 355 bp, respectively.

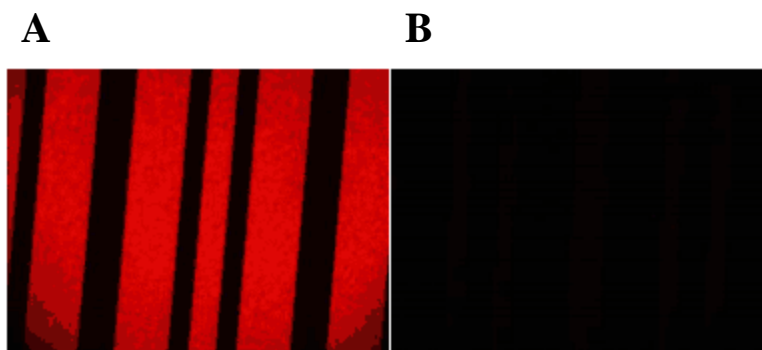


Figure 3.3. QC fluorescence. *Micrographs of fluorescence data for (A) specific target and (B) negative control hybridization assays imaged at 594 nm wavelength and 20X magnification.*

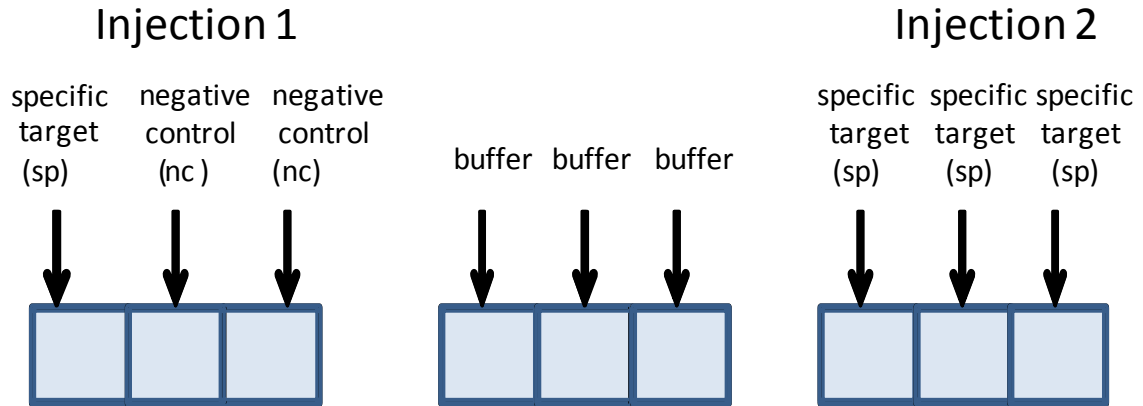


Figure 3.4. Adk assay diagram. Hybridization assays were done by first injecting specific (sp) target into chamber 1 and non-specific (nc) target into other two chambers. After buffer wash, all chambers were injected with sp target.

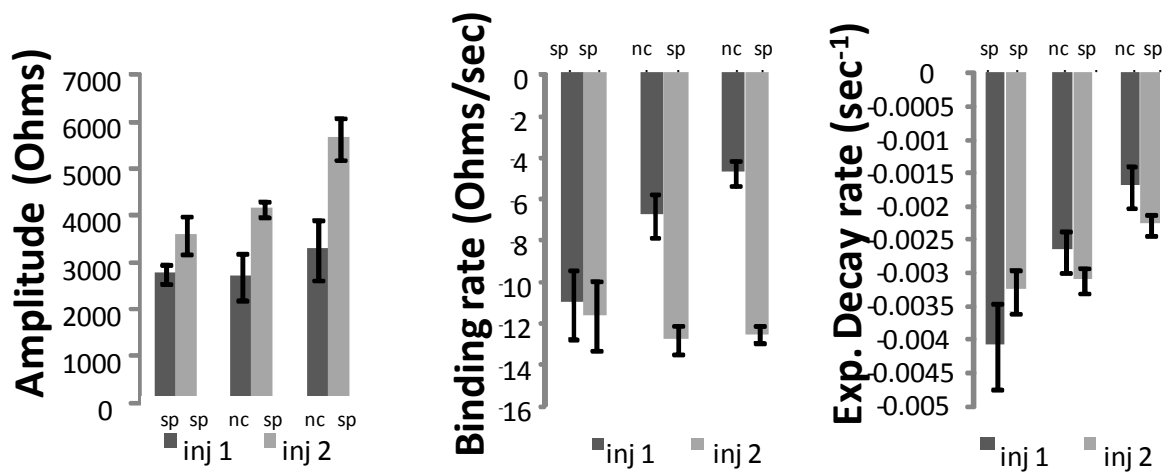


Figure 3.5. Adk hybridization assay. The binding curve parameters calculated for the complementary adk targets (sp) and non-complementary hly targets (nc) for injection 1 (dark grey) and injection 2 (light grey). Each bar is an average calculated from measurements of 5 different microelectrodes within a reaction chamber. Error bars indicate standard deviations.

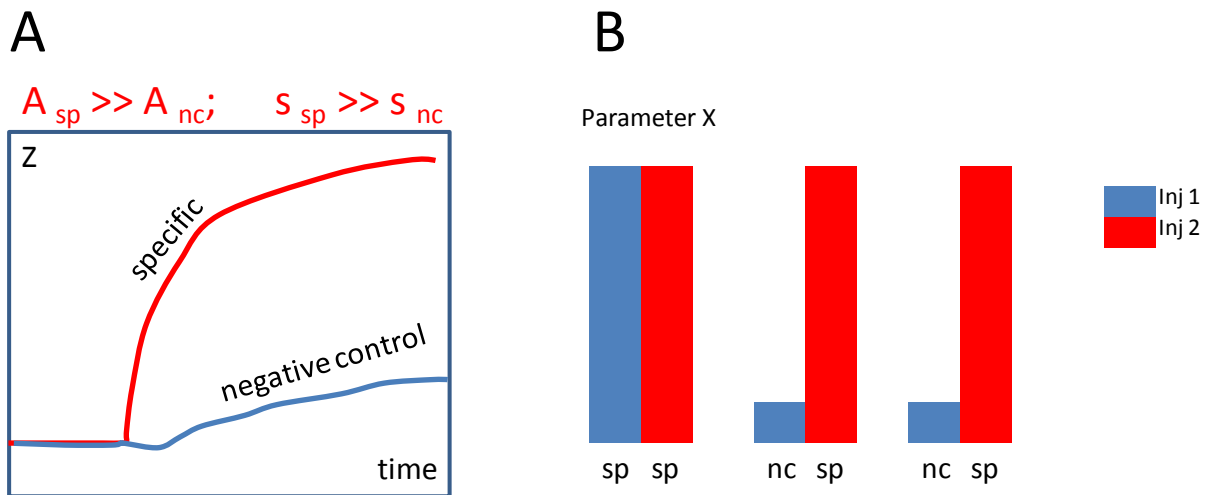


Figure 3.6. Idealized assay response. Binding curves of the normalized impedance signal (A) and binding curve parameter X (B) show idealized response for specific targets compared to negative controls; calculated parameters amplitude A and time constant s are significantly higher for specific injections compared to non-specific injections.

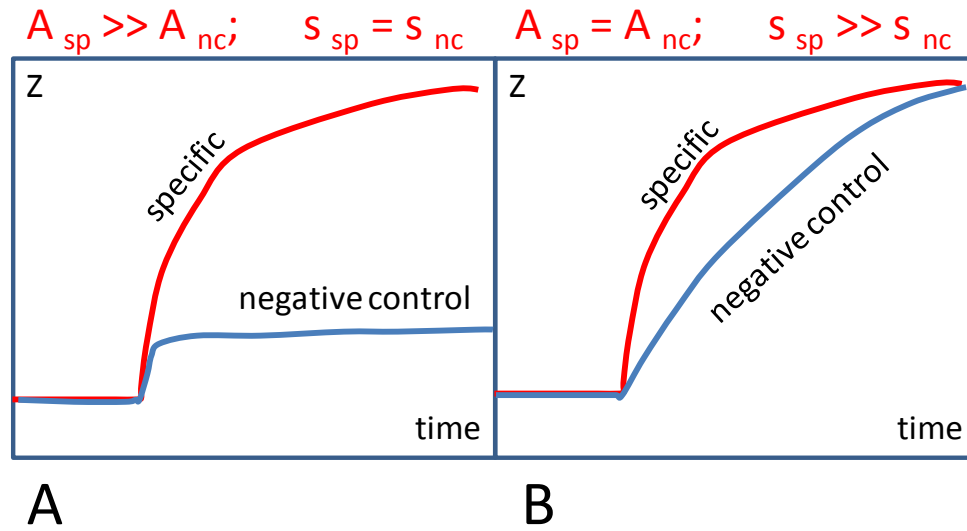


Figure 3.7. Alternative assay responses. (A) Binding parameter time constant s remains the same between injections 1 and 2, whereas amplitude A increases with second injection of specific target. (B) Time constant s increases from second injection of specific target, but amplitude A remains the same.

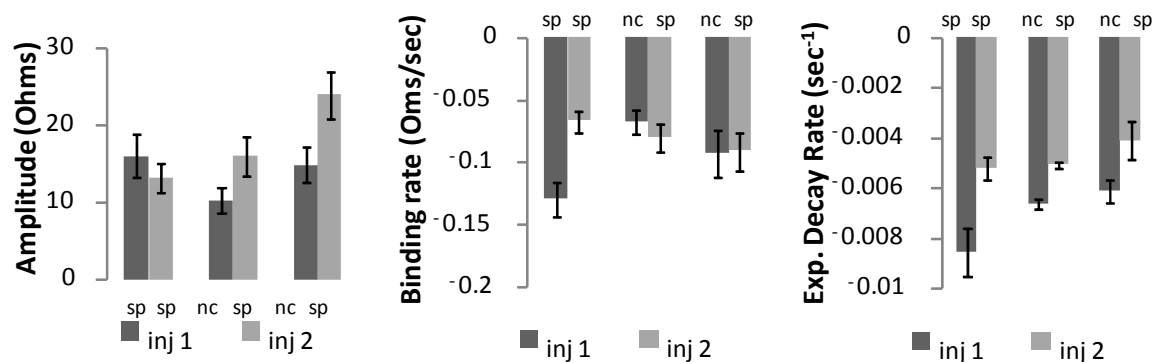


Figure 3.8. Assay with optimized frequency. *The binding curve parameters calculated for the complementary adk targets (sp) and non-complementary hly targets (nc) for injection 1 (dark grey) and injection 2 (light grey). Each bar is an average calculated from measurements of 5 different microelectrodes within a reaction chamber. Error bars indicate standard deviations.*

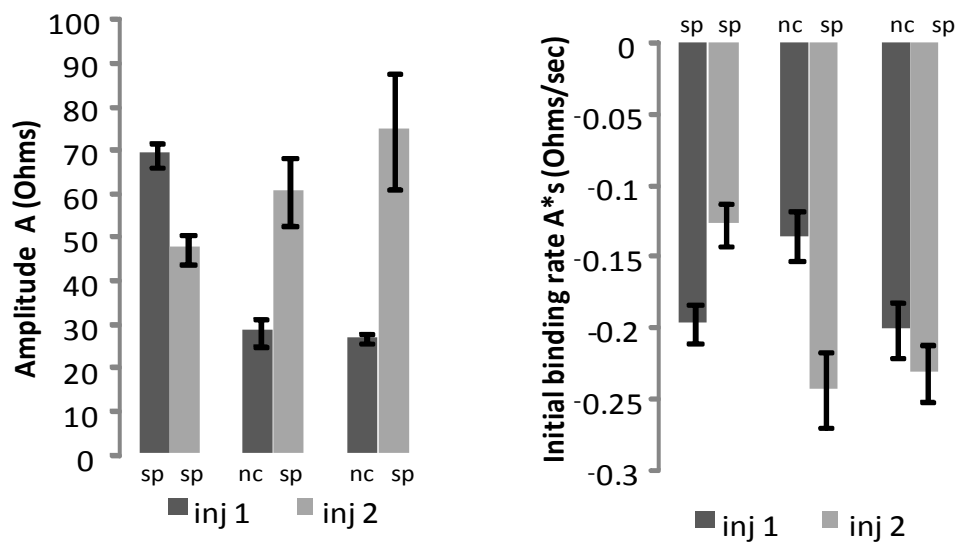


Figure 3.9. Adk assay optimization. The binding curve parameters calculated for the complementary adk targets (sp) and non-complementary hly targets (nc) for injection 1 (dark grey) and injection 2 (light grey). Each bar is an average calculated from measurements of 5 different microelectrodes within a reaction chamber. Error bars indicate standard deviations.

4. Enhancement of assay specificity

4.1 Introduction

4.1.1 Competition on array surface

Gene-specific detection methods are important for many applications, including environmental monitoring, disease prevention, and maintaining a high standard of food quality (Sen and Ashbolt 2011). Impedimetric assays are particularly advantageous because they rapidly produce real-time data of the presence and/or absence of targeted organisms. An important measure of specificity in genomic-based assays is differentiating between specific and non-specific targets within the same sample. For this reason, careful consideration of the negative controls used in a given study is essential. Probes used in genomic assays were complementary to three *E. coli* gene targets (*adk*, *hly*, and *stx*). The two targets non-complementary to the probe served as a negative control (e.g. the *hly* and *stx* targets are negative controls for the *adk* assays). For the *adk* assays, the *stx* target provided an excellent control because it shared no similarity to the *adk* probe (p-*adk*). In contrast, the *hly* target is partial-complementary to p-*adk*, resulting in cross-hybridization. Thus, assays specific for the *adk* target produced the largest difference in the impedance signal response for the *adk:stx* ratio in comparison to the *adk:hly* ratio (Chapter 2, Figure 2.3), suggesting that cross-hybridization with the *hly* target lowers the impedance signal for specific detection of the *adk* target. In addition to non-specific binding events that occur with negative controls, the dsDNA targets inherently renature after denaturation. This implies the target will either (1) bind to the probe on the sensor surface, (2) renature with its original anti-sense strand or (3) renature to a different anti-sense strand in solution. The latter two options reduce the number of target strands available for hybridization with the probe, thereby weakening the impedance signal for the specific target. Furthermore, the specific target could

bind to the probe in an unanticipated orientation, resulting in the formation of a secondary structure that could affect the impedance signal.

4.1.2 Enhancing assay specificity

Non-specific binding is a common problem in assay development that is mitigated by optimizing assay parameters. However, optimization requires time and does not always eliminate the issue (as with the *hly* target discussed in 4.1.1). We speculate that a number of different interactions occurred on the sensor surface. Therefore, the best approach for eliminating non-specific binding is to improve the probe:specific target interaction. To enhance assay specificity, we modified surface functionalization with multiple probes to allow more target binding opportunities. Multiple probe sets contain a mixture of probes that have different complementary regions to the target; thus, probe:target hybridization events are more diverse than those with binding to a single probe (e.g., one target strand binds in two places on the probe or both target strands bind to two individual probes). Arrays containing probes that have two regions corresponding to the specific target increases the hybridization efficiency compared to those with only one complementary region because the target has amplified affinity for the probes. We hypothesized that an amplified affinity between the target and probe would increase the impedance signal response by increasing both the rate and extent of hybridization events. Furthermore, target:probe binding creates a double-stranded complex that has a unique melting temperature (T_m), which can be exploited to give an accurate measure of the specificity of the hybridized complex. Therefore, assay specificity can be improved by analyzing melting curve data. To reduce complications associated with dsDNA targets (as described above), we measured the melting curves of ssDNA targets.

4.1.3 Aims of this study

Our previous results demonstrated that the SLA impedimetric platform detects gene-specific *E. coli* targets. Here we built on prior work by enhancing assay specificity through use of multiple DNA probes for each target gene and assay optimization. We hypothesized that different functionalization techniques would show different patterns of DNA-DNA binding. In addition to this multiple probe study, we aimed to improve assay resolution by analyzing the melting curves for each hybridization interaction, enabling a three-dimensional picture of hybridization (Z, time and temperature). My thesis research included DNA target preparations, performing hybridization and melting curve assays and data analysis.

4.2 Materials and Methods

4.2.1 Multiple probes

Sensor arrays were functionalized using oligonucleotide probes that were thiol-modified on the 5' end for attachment to surface electrodes. The following probes were designed from *E. coli* target amplicons: (1) p-*adk*-1, 5'-TGGAGAAATATGGTATTCCG-3', (2) p-*adk*-3, 5'-AAGACATTATGGATGCTGG-3' and (3) p-*adk*-3rev, 5'-CCAGCATCCATAATGTCTT-3'. Sensor arrays were functionalized with either: (1) a single p-*adk*-1 probe; (2) a 1:1 mixture of p-*adk*-1 and p-*adk*-3 [designated 1-3]; or (3) a 1:1 mixture of p-*adk*-1 and p-*adk*-3rev [designated 1-rev]. The 1-3 probe set was complementary to two different regions on the target sense strand. The 1-rev probe set contained two individual probes complementary to either the target sense strand or the target anti-sense strand (**Figure 4.1**). Both multiple probe sets provided more than one sequence for the intended target to bind, whereas the single *adk* probe contained one complementary sequence for target sense strand binding.

4.2.2 DNA target preparation

Double-stranded DNA target preparation was described in detail in section 2.2.4. Briefly, dsDNA targets were prepared by PCR using gene-specific primers for *adk* and *stx* genes (Chapter 2, Table 2) and genomic *E. coli* DNA. Post-PCR, amplicons were purified using QIAquick PCR Purification Kit (Qiagen, Valencia, CA) and dsDNA concentrations analyzed using a NanoDrop spectrophotometer (Thermo Scientific, Wilmington, DE). DNA targets were denatured at 95°C for 5 min prior to immediate injection into sensor chambers for multiple probe experiments.

4.2.3 Hybridization and optimization using multiple probes

Detection of the *E. coli adk* gene was performed on sensor arrays functionalized with single (p-*adk*-1) or multiple probe sets (1-3 or 1-rev). Targets were hybridized in buffer of 1x SSPE with 0.1% Triton X100 at 42°C. The target concentration was optimized by testing 0.01, 0.1 and 0.3 $\mu\text{g}\cdot\text{ml}^{-1}$. Impedimetric measurements were carried out at 24 Hz and 100 mV. Target-free buffer was injected into chambers to establish a baseline impedance value, after which complementary (*adk*) dsDNA target was injected into two chambers and non-complementary (*stx*) dsDNA target into the remaining chamber.

Assays using multiple probes were optimized by testing a range of temperatures (30-50 °C). A temperature gradient also provided a useful comparison of impedance signals achieved by probe:target hybridization for multiple and single probe assays. Hybridization of the complementary target to the array resulted in a binding curve, and the metrics amplitude *A* and time constant *s* were calculated and averaged from the exponential curve fit of 5 electrodes (theoretical fit shown in **Figure 4.2**). *A* and *s* values for specific target binding were averaged and used for comparison of different probe sets.

4.2.4 Temperature control system

A real-time temperature control system (developed by Mike Frasier at SLA) provided controlled heating and cooling to the hybridized sensor surface and maintained electrical communication with the IA-2 impedance analyzer. The temperature control system was modified with a peltier heat exchanger (TE Technology, Traverse City, MI) attached to an aluminum block and machined to fit the sensor array platform. The peltier device was powered through a high current power supply with thermocouple feedback. The system was controlled by a proportional-integral-derivative (PID) device and a TE Technology TC-36-25 RS232 temperature controller (Traverse City, MI). Instead of the standard 3-cell chamber, the fluidic interface consisted of a single acrylic chamber fitted to the sensor array surface and sealed with a Viton gasket (Apple Rubber Products, Lancaster, NY). The single chamber encapsulates all 15 electrodes in a common aqueous environment; however, each electrode was monitored independently. The temperature control system was used for melting curve assays.

4.2.5 Melting curve assays

Impedimetric signals for probe:target hybridization was measured on all 15 electrodes during two periods of temperature cycling: (1) temperature was increased from 30 to 80 °C at a rate of 4° per sec, and (2) temperature was decreased from 80 to 30 °C at a rate of 2° per sec. Both periods cycled into and out of the probe:target denaturation temperature zone (57-60 °C). Assays were performed on the same array in a two-step process: (1) buffer or non-specific *hly* target injection followed by (2) specific *adk* target injection. Sensor arrays functionalized with p-*adk* were hydrated with 2x SSPE buffer for one hour. After a baseline measurement was obtained with buffer alone, sensor arrays were incubated with 0.1 ug·mL⁻¹ ssDNA targets for 20 min. The ssDNA targets were generated by *in vitro* transcription (described in detail in Chapter 3.2.1) and received no treatment prior to injection into sensor chamber. Voltage and frequency were set at

25 mV and 480 Hz, respectively, and real-time impedance measurements were extracted by the mathematical algorithm. The first derivative of the impedance signal ($\Delta Z/\Delta t$) was averaged and melting curves were analyzed by evaluating disruptions in the $\Delta Z/\Delta t$ response for temperature increase and decrease periods.

4.3 Results and Discussion

4.3.1 Multiple probes improve assay specificity

We tested the hypothesis that impedimetric specificity to the *adk* target improves with multiple probe:target interactions. Hybridization assays were performed on sensor arrays functionalized with three different probe sets (single [p-*adk*] and multiple [1-3 and 1-rev] probes) for specific detection of the *adk* dsDNA target; whereas the *stx* dsDNA target served as the negative control. A mathematical algorithm extracted exponential curve parameters amplitude A , time constant s , binding rate $A*s$ and the integrated area for comparison of the sensor signal response among probe sets. For all probe sets the preliminary results indicated that the binding parameters were not significantly different for the *adk* target compared to the negative control (data not shown). Additionally, the impedance response for the *adk* target did not change significantly with hybridization to different probe sets. Therefore, assay optimization was needed to improve differentiation of specific and non-specific target binding signals. Hybridization temperature was optimized to improve the assay and used for comparison of all three functionalization techniques.

4.3.2 Optimized multiple probe assays

Binding curve parameters for detection of the *adk* and *stx* targets were compared using three different probe sets at different temperatures (30, 34, 42, 45 and 50 °C). Optimization of assay temperature revealed significant differences in the impedance signal; amplitude A and time

constant s showed higher values for complementary (adk) compared to non-complementary (stx) binding. Additionally, A and s averaged across independent assays for adk binding indicated that the orientation of binding affects the impedance signal (**Figures 4.3** and **4.4**, respectively). In hybridizations with the 1-3 probe set, amplitude A appeared to be relatively temperature-independent, while hybridization to the single and 1-rev probes appeared to increase with increasing temperature. Binding curve parameter binding rate $A*s$ showed similar results to amplitude for hybridization with the 1-3 probe set, remaining fairly constant with increasing temperature, and both single and 1-rev probe sets showed highest values at highest temperatures. Additionally, the integrated area was highest at the highest temperature for binding to all three probe sets (**Figure 4.5**). Therefore, hybridization to the 1-3 probe set was relatively constant with increasing temperature for three out of four assay parameters. The 1-3 probe set provides two different complementary regions for target sense strand binding. This binding pattern may form a non-linear hybridized complex on the array surface, limiting the exposure of the biomolecules (responsible for changing array surface properties) to the aqueous environment, thereby reducing impedance signals.

Overall, the highest signal response was obtained using 1-rev probes at 50°C. The temperature trends for single and 1-rev probes were similar for A and s values; however, the magnitude of the A and s values for 1-rev probes were generally higher than those with the single probes. These data suggested the SLA sensor array assay may be improved using the 1-rev probe set at 50°C. We speculated that the hybridization of both target strands with the 1-rev probes improved the impedance signal response because both target strands hybridized with the probes in a linear orientation, therefore remained in the aqueous environment. In addition, the 1-rev probes may have improved the impedance signal response because they provided greater

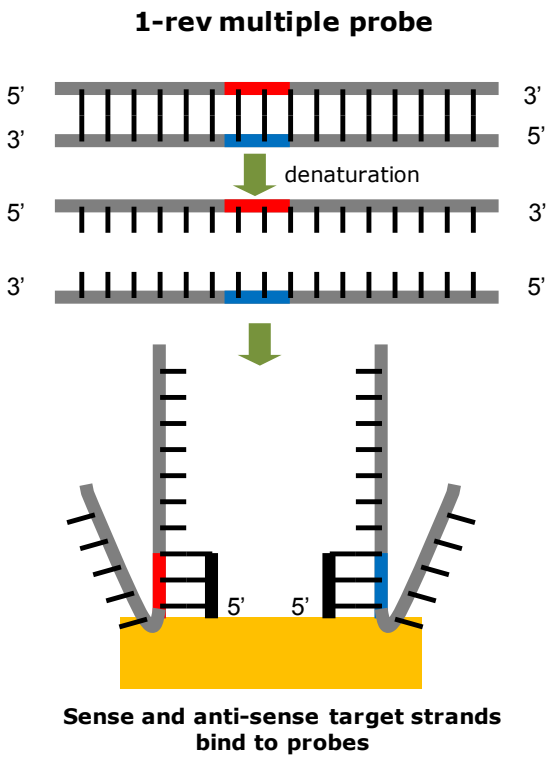
sequence coverage of the targeted gene and therefore reduced the rate of target renaturation. Additionally, the p-*adk*-3rev probe could simply have had a greater hybridization efficiency compared to the other probes. Thus, our results demonstrated that the impedance signal response was enhanced by optimizing assay conditions and possibly providing more target binding opportunities with the 1-rev probes.

4.3.3 Melting curve analysis

The melting curve for specific (*adk*) ssDNA target:probe hybridization was compared to that for injections of buffer alone and for hybridization with the non-specific (*hly*) target. Binding curve data (impedance/time) was extracted as temperature cycled and a first derivative of the impedimetric signal ($\Delta Z/\Delta t$) was calculated to determine changes in hybridization events. We expected to see a depressed peak in the first derivative as temperature increased, indicating dissociation of the hybridized target and probe complex (**Figure 4.6**). As temperature decreased, we expected to see a raised peak in the first derivative response indicative of a hybridization event. The first derivative of the impedimetric response showed a depressed peak with *adk* when compared to a flat line in the buffer. However, *hly* also showed a similar peak, though smaller in magnitude (**Figure 4.7**). The peak associated with *adk*:probe denaturation appeared to be within the melting temperature range for the ssDNA target ($T_{m_{adk}} = 57-60^{\circ}\text{C}$). Additionally, as temperature decreased, the $\Delta Z/\Delta t$ showed an elevated peak within the calculated melting temperature range for *adk*, suggesting a specific target:probe interaction had occurred (**Figure 4.8**). The signal response for buffer alone remained relatively flat as temperature decreased. A repeat of the experiment comparing *adk* and *hly*, however, did not yield similar results. Neither of the melting curves for *adk* and *hly* indicated disruptions in the signal as temperature decreased. Additionally, all experiments showed a high level of noise in the data, implying an

engineering error in the control of temperature within the melting curve system. The rates of temperature increase and decrease for these experiments were 4°C/sec and 2°C/sec, respectively. We predict these rates are too fast for analysis of a first derivative response, and that consequently we may be missing the dissociation/re-association events (melting curve peaks). Furthermore, when the rate of temperature change drops to zero (i.e., no change), these spots seem to correspond to peaks associated with noise (data not shown). These data suggested melting curve experiments require extensive improvement by SLA in engineering and data analysis. Our result showing idealized peaks for *adk* suggested this method may greatly improve assay resolution and specificity for specific target:probe hybridization events on the sensor array surface in the future.

(A)



(B)

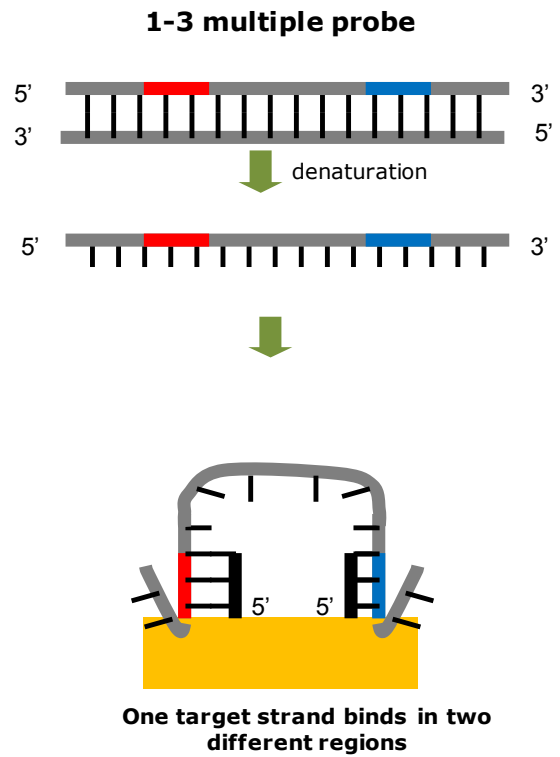


Figure 4.1. Multiple probe functionalization techniques. *Illustration of two multiple probe functionalization techniques. (A) 1-rev probes and (B) 1-3 probes. In 1-rev approach, probes have complementary sequences to both sense and anti-sense strands of dsDNA target. In 1-3 approach, both probes have differing complementary sequences to the sense strand of dsDNA target, allowing for target binding in two different regions (green and blue regions).*

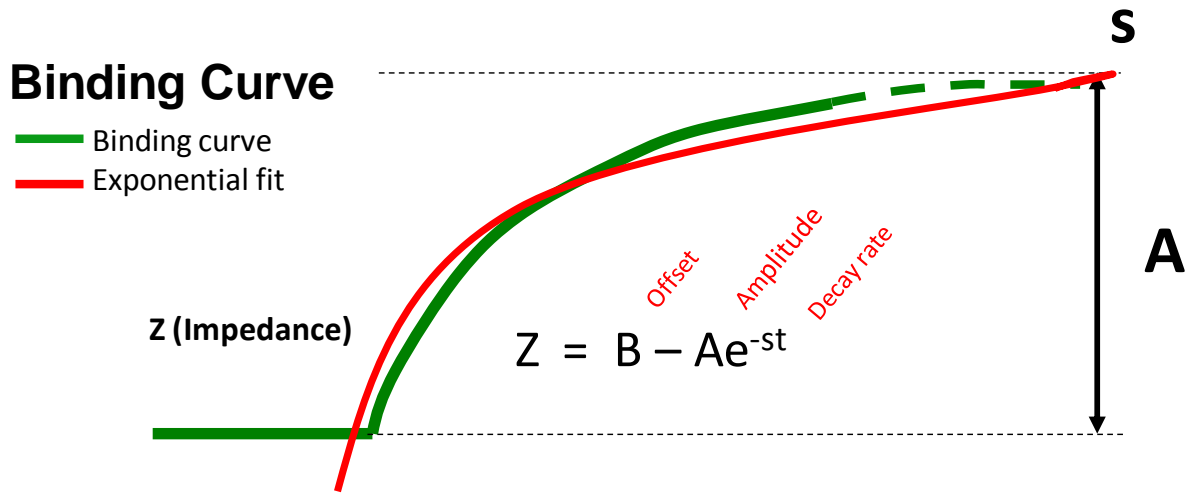


Figure 4.2. Data analysis algorithm. Analysis of impedimetric binding curve. Integrated mathematical algorithm extracts the parameters amplitude A and time constant s from theoretical exponential decay plot.

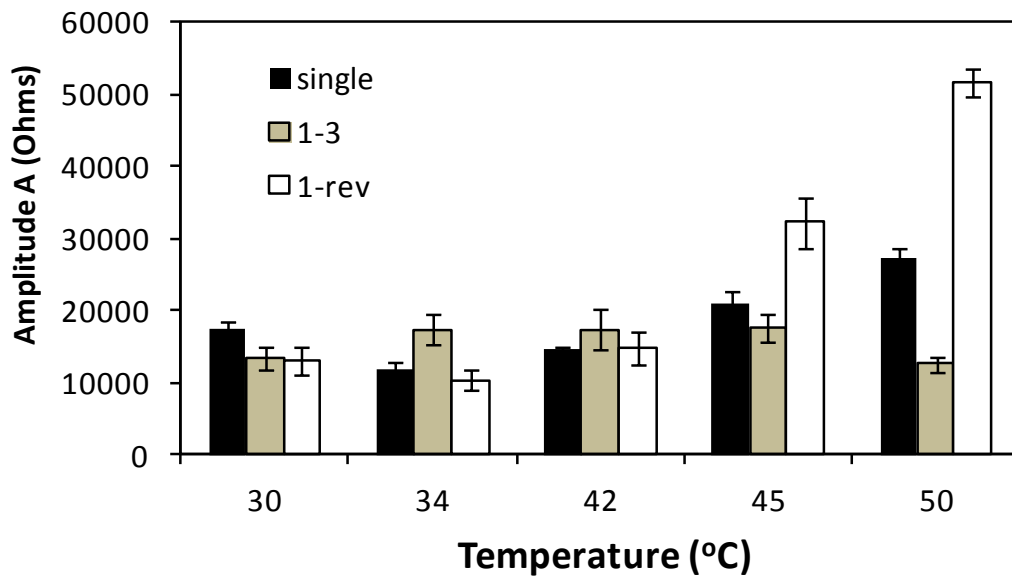


Figure 4.3. Amplitude of *adk*:probe binding. Binding curve parameter amplitude A (Ohms) for specific (*adk*) target:probe hybridization for single (black bars), 1-3 (grey bars) and 1-rev (white bars) probes at different temperatures. Each bar represents the averaged amplitude from independent experiments ($n=6$); error bars indicate standard deviations.

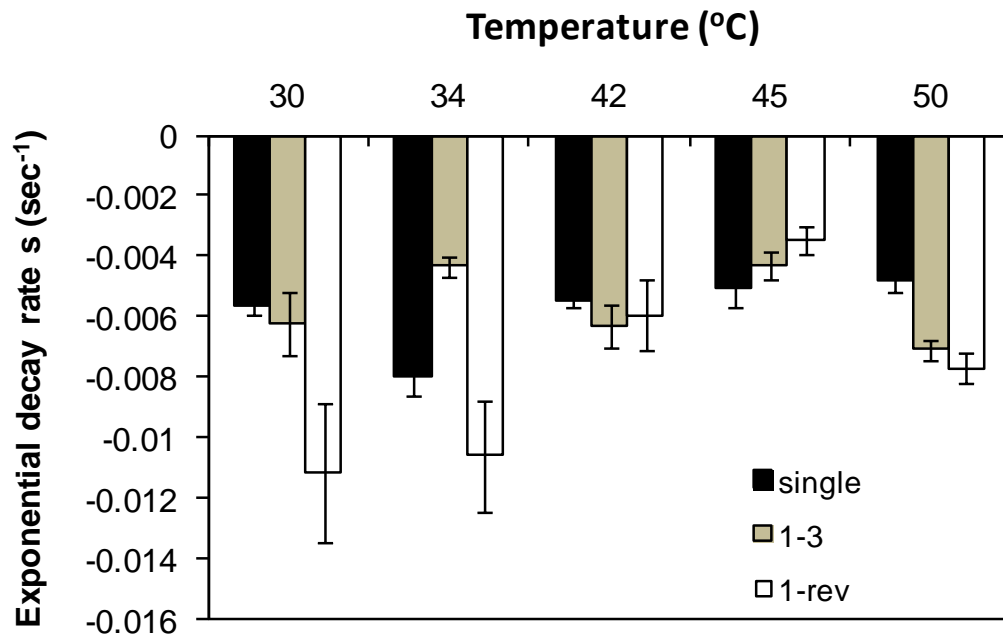


Figure 4.4. Exponential decay rate of *adk*:probe binding. Binding curve parameter exponential decay rate s (sec^{-1}) for specific (*adk*) target:probe hybridization for single (black bars), 1-3 (grey bars) and 1-rev (white bars) probes at different temperatures. Each bar represents the averaged amplitude from independent experiments ($n=6$); error bars indicate standard deviations.

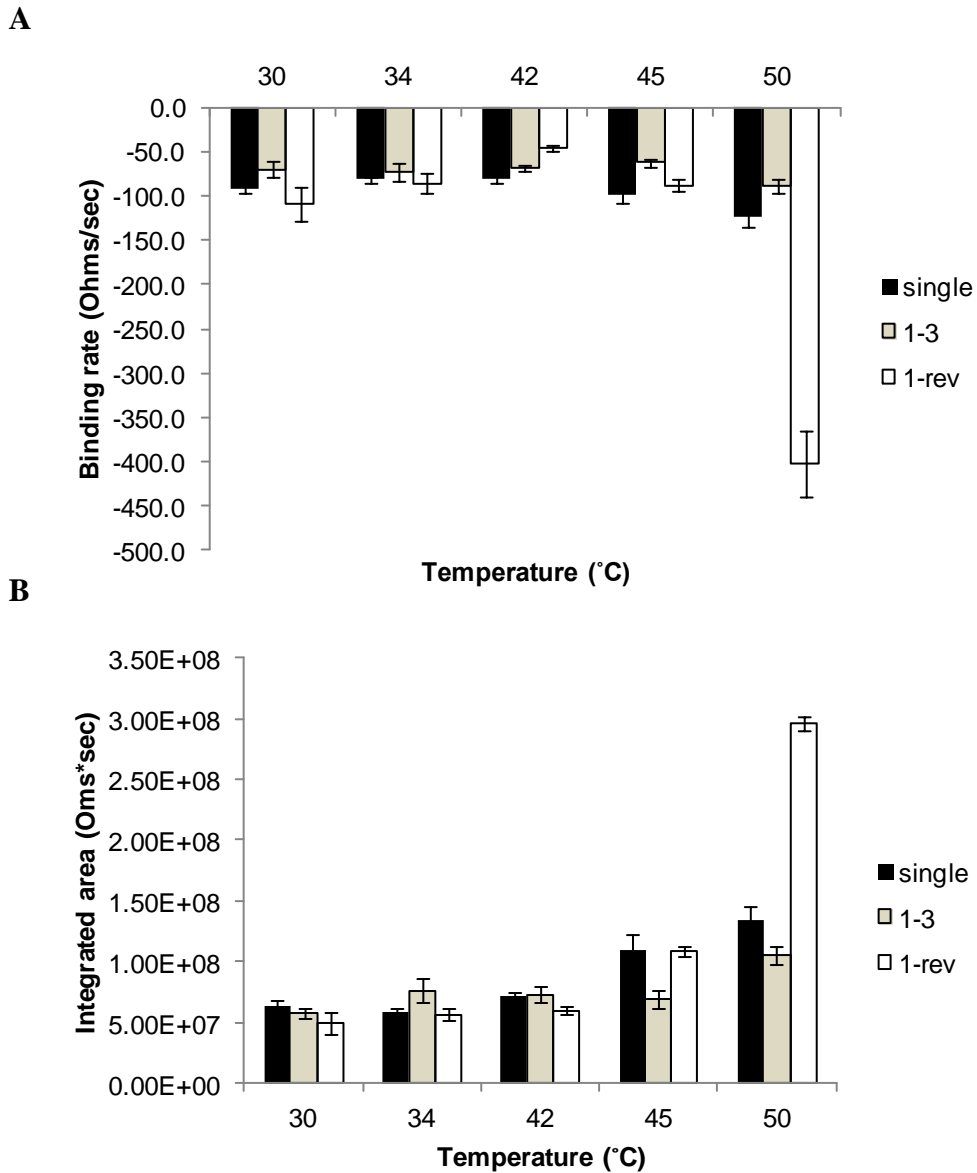
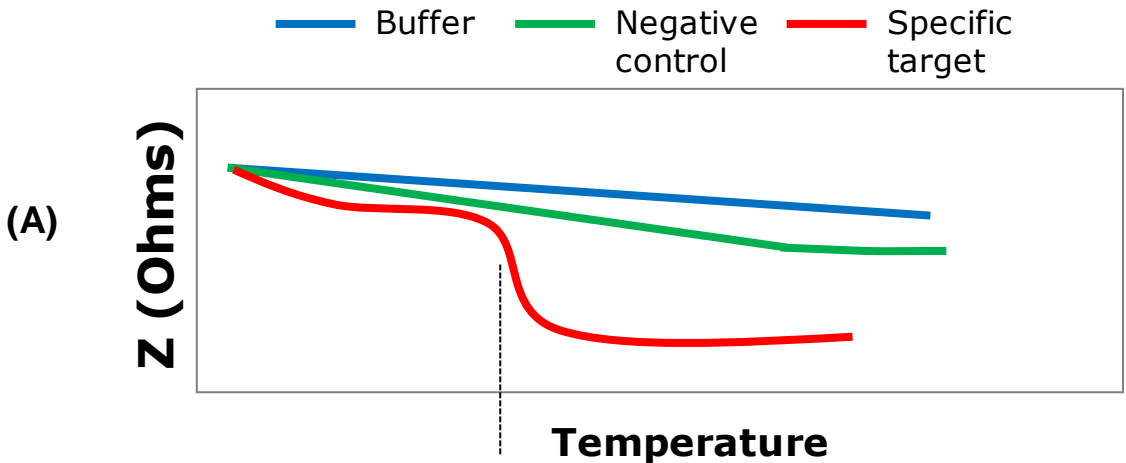
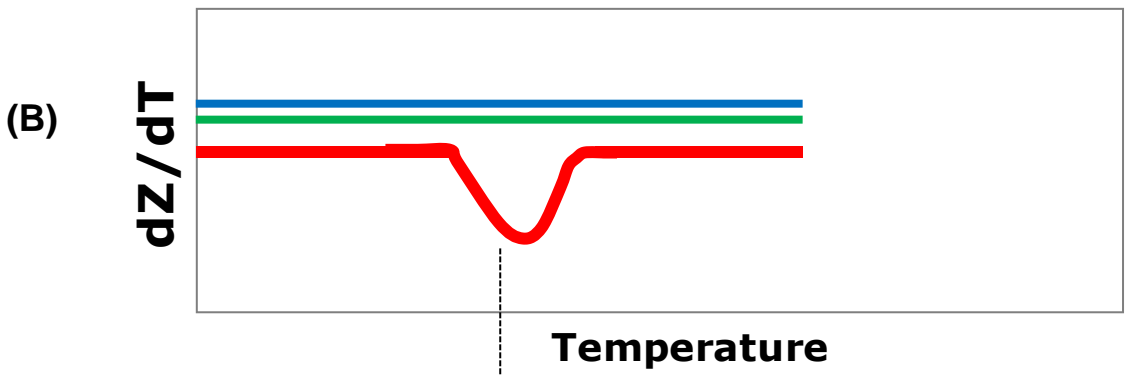


Figure 4.5. Binding rate and integrated area of *adk*:probe binding. Binding curve parameters binding rate (A) and integrated area (B) for specific (*adk*) target:probe hybridization for single (black bars), 1-3 (grey bars) and 1-rev (white bars) probes at different temperatures. Each bar represents the averaged amplitude from independent experiments ($n=6$); error bars indicate standard deviations.



Melting temperature (T_m)



Melting temperature (T_m)

Figure 4.6. Idealized melting curve. *Idealized melting curve for temperature increase experiments. (A) change in impedance (Z) as melting temperature of hybridized complex is reached and (B) melting temperature produces a depressed peak in first derivative impedance response.*

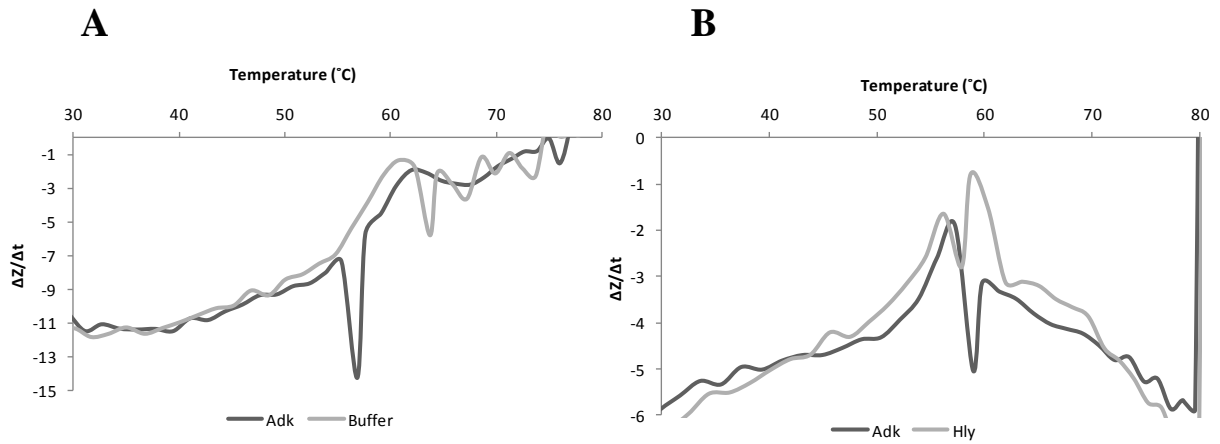


Figure 4.7. Melting curves associated with increasing temperature. *Change of impedance (Z) over time (sec) with increasing temperature. (A) shows the melting curves for buffer alone (grey) and for hybridization with the specific adk (black target; (B) shows the melting curves for the non-specific hly (grey) and specific adk (black) targets.*

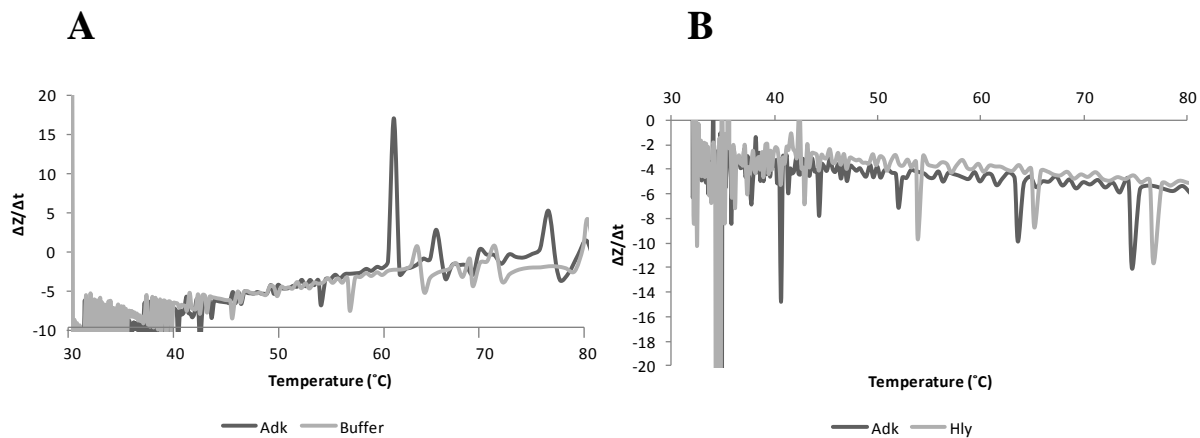


Figure 4.8. Melting curves associated with decreasing temperature. Change of impedance (Z) over time (sec) with decreasing temperature. (A) shows the melting curves for buffer alone (grey) and for hybridization with the specific adk (black) target; (B) shows the melting curves for the non-specific hly (grey) and specific adk (black) targets.

5. Conclusions and Future Directions

5.1 Genomic DNA-based assay development

My thesis research involved developing a genomic DNA-based assay for rapid characterization of pathogens in the environment. SLA developed an impedimetric biosensor platform, which was capable of distinguishing *E. coli* strains using short PCR-amplified oligonucleotide targets. In order to use this platform in environmental monitoring applications, we developed a genomic-based assay using full-length PCR-amplified DNA targets. Hybridization assays were performed on sensor arrays functionalized with gene-specific probes. Double-stranded DNA targets were amplified from three gene (*adk*, *hly* and *stx*) fragments from different *E. coli* strains. The use of dsDNA targets streamlined target preparation because post-PCR processing was minimal, unlike assays using ssDNA targets. Calculated binding curve parameters of the impedance signal response were used to analyze specific target binding compared to cross-hybridization of negative controls.

Our results demonstrated that the SLA platform could effectively differentiate *E. coli* strains with gene-specific probes. Furthermore, extensively optimizing hybridization assays significantly improved the impedimetric signal response for the specific target. These results highlighted the need for optimizing each gene-specific assay (for *adk*, *hly* and *stx*) independently with careful consideration of negative controls. My thesis research for this study led to the Ghindilis *et al.*, 2012 publication.

The SLA impedimetric platform is capable of detecting DNA-DNA hybridization in real-time and is a robust method for specific detection of pathogenic microorganisms. In environmental samples, analyte concentrations tend to be extremely low and are present in complex media. Therefore, gene-based assays with environmental samples require higher

specificity than assays performed in homogenous media. In typical environmental surveys, specific targets are often present at low abundance, therefore PCR amplification is necessary for their detection. For these reasons, we plan to integrate a real-time PCR unit with the SLA impedimetric biosensor to reduce sample processing time and alleviate the problem associated with low pathogen abundance in the environment.

5.2 Universal sensor array

An important goal for CMOP is to develop an integrated, user-friendly, automated biosensor for high-resolution monitoring of the Columbia River. The SLA impedimetric detection system is amenable for field sampling for a number of reasons: it is inexpensive, it performs real-time analyses, and it is mechanically simple. In order to improve the marketability of the SLA platform for a variety of applications including environmental monitoring, SLA conceptualized a novel pre-functionalization technique that would allow individual users to develop their own independent assays. We aimed to develop a hybridization assay for rapid detection of full-length ssDNA targets as an initial step towards RNA detection, while at the same time testing the new SLA pre-functionalization technique. Our results validated the use of the SLA platform for detection of ssDNA gene targets, and by optimizing stimulation frequency and voltage we were able to reduce the negative impact of cross-hybridization signals on the measured signal response for specific targets.

The detection of ssDNA targets laid the way for real-time detection of RNA targets, which is particularly important for pathogen monitoring and risk assessment because gene transcripts (messenger RNA [mRNA]) provide information about cellular activity. The translation of mRNA into proteins requires the participation of rRNA. Detection of rRNA is advantageous because it does not require target amplification because active cells produce a

large number of rRNA transcripts, which are themselves involved in protein synthesis. Thereby in theory, target preparation steps are fewer for the detection of RNA compared to the detection of DNA. Future directions are to develop an assay for detection of *E. coli* RNA targets using probes that are complementary to the anti-sense RNA strands. This study also displayed poor assay reproducibility and trouble-shooting is needed to correlate QC fluorescence data with impedimetric measurements from hybridization assays to ensure uniform functionalization of sensor arrays.

5.3 Enhancement of assay specificity

Previous hybridization assays with dsDNA targets showed that extensive optimization was necessary to distinguish the assay signal response for specific and non-specific targets (Chapter 2; Ghindilis *et al.*, 2012). We speculated that competitive binding reactions (i.e., renaturation) negatively influenced the impedance signals for specific target binding by reducing the amount of target sense strands available to bind to the probes. Therefore, we attempted to enhance assay specificity by utilizing multiple probes and incorporating melting curve data.

The results comparing the signal response for different probe sets illustrated the effect of temperature on DNA-DNA binding. The 1-rev probe set (with binding sites for both target sense and anti-sense strands) revealed higher signal response with increasing temperature and better target discrimination in comparison to the single probe set. This probe set improved specificity and may have eliminated processes in the aqueous environment that diminished the impedance signals (e.g., renaturation of the dsDNA target) by providing an additional probe complementary to the target anti-sense strand. The 1-3 probe set (with two independent sites for target sense strand binding) appeared to be relatively temperature insensitive and did not improve the assay signal response. Although the 1-3 probe set did not appear to enhance the assay signal response,

it could be applied in the development of real-time PCR directly on the sensor array surface (necessary for DNA detection) precisely because the signal response does not appear to change with increasing temperature. Further experimentation is needed to determine the reliability of the 1-3 probe set at the extreme temperatures required for PCR (i.e., 95° C). Another potential use for the 1-rev and 1-3 probe sets is in haplotyping, which is used to investigate whether two sites are present on the same target strand or on two separate strands. Because the results of target binding to 1-rev and 1-3 probe sets revealed different characteristics with increasing temperature, discrimination between binding of separate target strands and binding of two regions of the same target strand is possible.

Results from the melting curve experiments showed that monitoring of the dissociation and re-association events between probe and target led to differentiation between specific binding and cross-hybridization. Although our results were highly variable, melting curve data have the potential to improve assay resolution. Future plans include improving assay accuracy and reproducibility by incorporating a melting curve data algorithm into the SLA instrument and improving the engineering of the temperature control system. Altering the design of the sensor array surface so that the aqueous environment is constantly mixing would facilitate more efficient thermodynamic cycling and guarantee homogenous heating and cooling of the hybridized probe:target complexes. In addition, better control of the temperature change rate would allow optimization of the melting curve assay.

Finally, long-term plans include further miniaturization and automation of the SLA platform using an injection system that would synchronize with the instrument reader. The current limitations of the SLA impedance biosensor are its size, lack of reproducibility between and within sensor arrays, the extensive optimization required for the detection of PCR-amplified

targets and the absence of an integrated PCR module for amplification of specific DNA targets (essential for detection of environmental DNA). Therefore, incorporating a microfluidics block for real-time PCR would result in a device that is suitable for rapid field-use and environmental monitoring of DNA targets. However, the requirement for PCR can be eliminated by focusing on the detection of rRNA targets that are abundantly transcribed in active cells. We aim to incorporate the SLA impedimetric platform into the ESP, which in conjunction with the ESP core device will allow for autonomous sample collection, processing and *in situ* impedimetric assays. This integrated device will have the capability for adaptive sampling, which triggers sampling events when pre-programmed thresholds for specific environmental parameters are met.

Real-time detection has major advantages over end-point detection because it allows for simultaneous data extraction and analysis of binding events. The impedimetric signals produced from probe:target hybridization events and the analytical fitting of the binding curve together provide rapid determination of the specificity of a target. However, because the impedimetric output is a sum of all the changes in surface chemistry, discrimination between specific and non-specific target binding is a major challenge for label-free assay methods. Although my research improved assay specificity, the need for (1) individual assay optimization and (2) significant improvement in assay reliability was indicated. In the end, we successfully illustrated the application of genomic-based assays using the SLA platform, while also providing SLA with useful information needed for future developments of their platform. Altogether, the SLA impedimetric biosensor is capable of detection of microbial pathogens in near real-time and with future improvements will be a suitable device for environmental monitoring.

6. References

- Akinyemi, K.O., A.O. Oyefolu, B. Opere, V.A. Otunba-Payne and A.O. Oworu, 1998. *Escherichia coli* in patients with acute gastroenteritis in Lagos, Nigeria. *East African Med J.* **75**:9, 512-515.
- Altman, B., C. M. Henson, I. R. Waite, 1997. Summary of information on aquatic biota and their habitats in the Willamette Basin, Oregon, through 1995. *USGS Survey*, <http://hdl.handle.net/1957/4863>. Accessed July 4, 2013.
- Barreiros dos Santos, M., J. P. Aguil, B. Prieto-Simon, C. Sporer, V. Teixeira and J. Samitier, 2013. Highly sensitive detection of pathogen *Escherichia coli* O157:H7 by electrochemical impedance spectroscopy. *Biosensors and Bioelectronics*, **45**, 174-180.
- Belt, K.T., C. Hohn, A. Gbakima, and J.A. Higgins, 2007. Identification of culturable stream water bacteria from urban, agricultural, and forested watersheds using 16S rRNA gene sequencing. *J. of Water and Health* **5**: 395-406
- Beutin, L., S. Jahn and P. Fach, 2009. Evaluation of the 'GeneDisc' real-time PCR system for detection of enterohaemorrhagic *Escherichia coli* (EHEC) O26, O103, O111, O145 and O157 strains according to their virulence markers and their O- and H-antigen-associated genes. *J. Appl. Microbiol.* **106**: 4, 1122-1132.
- Blattner, F. R., G. Plunkett III, C. A. Bloch, N. T. Perna, V. Burland, M. Riley, J. Collado-Vides, J. D. Glasner, C. K. Rode, G. F. Mayhew, J. Gregor, N. W. Davis, H. A. Kirkpatrick, M. A. Goeden, D. J. Rose, B. Mau and Y. Shao, 1997. The complete genome sequence of *Escherichia coli* K-12. *Science* **277**: 5331, 1453-1462.
- Brichta-Harhay, D. M., T. M. Arthur, J. M. Bosilevac, M. N. Guerini, N. Kalchayanand and M. Koochmaraie, 2007. Enumeration of *Salmonella* and *Escherichia coli* O157:H7 in ground beef, cattle carcass, hide and faecal samples using direct plating methods. *J. Appl. Microbiol.* **103**: 5, 1657-1668.
- Buchanan, R. L. and M. P. Doyle, 1997. Foodborne disease significance of *Escherichia coli* O157:H7 and other enterohemorrhagic *E. coli*. *Food Technol.* **51**: 10, 69-76.
- Call, D. R., M.K. Borucki and F.J. Loge, 2003. Detection of bacterial pathogens in environmental samples using DNA microarrays. *J. Microbiol. Methods* **53**:2, 235-243.
- Chen, J., N. Chang, M. ASCE, C. Chen, and C. Fen, 2004. Minimizing the ecological risk of combined-sewer overflows in an urban river system by a system-based approach. *J. of Environ. Eng.* **130**: 1154-1169
- Daniels, J. S. and N. Pourmand, 2007. Label-free impedance biosensors: opportunities and challenges. *Electroanalysis* **19**: 12, 1239-1257.
- Doucette, G. J., C. M. Mikulski, K. L. Jones, K. L. King, D. I. Greenfield, R. Marin III, S. Jensen, B. Roman, C. T. Elliott and C. A. Scholin, 2009. Remote, subsurface detection of the

algal toxin domoic acid onboard the environmental sample processor: assay development and field trials. *Harmful Algae* **8**: 6, 880-888.

Ghindilis, A. L., M. W. Smith, K. R. Schwarzkopf, C. Zhan, D. R. Evans, A. M. Baptista and H. M. Simon, 2009. Sensor array: impedimetric label-free sensing of DNA hybridization in real time for rapid, PCR-based detection of microorganisms. *Electroanalysis* **21**: 13, 1459-1468.

Ghindilis, A. L., K. R. Schwarzkopf, D. S. Messing, I. Sezan, P. Schuele, C. Zhan, M. W. Smith, H. M. Simon and D. R. Evans, 2010. Real-time biosensor platform: fully integrated device for impedimetric assays. *ECS Transactions* **33**: 8, 59-68.

Ghindilis, A. L., 2011. Impedance spectroscopy measurement of DNA. *European Patent Application*, EP2342332.

Ghindilis, A. L., M. W. Smith, D. S. Messing, V. N. Haynes, G. B. Middleton, K. R. Schwarzkopf, C. E. Campbell, C. Zhan, B. Ulrich, M. J. Frasier, P. J. Schuele, D. R. Evans, I. Sezan, J. W. Hartzell and H. M. Simon, 2012. Development of real-time assays for impedance-based detection of microbial double-stranded DNA targets: optimization and data analysis. *Biosensors and Bioelectronics* **35**: 1, 87-93.

Greenfield, D. I., R. Marin III, S. Jensen, E. Massion, B. Roman, J. Feldman and C. A. Scholin, 2006. Application of environmental samples professor (ESP) methodology for quantifying *Pseudo-nitzschia australis* using ribosomal RNA-targeted probes in sandwich and fluorescent *in situ* hybridization formats. *Limonol. and Oceano.:Methods* **4**, 426-435.

Hajnsdorf, E., O. Steier, L. Coscoy, L. Teyssset and P. Regnier, 1994. Roles of RNase E, RNase II and PNPase in the degradation of the rpsO transcripts of *Escherichia coli*: stabilizing function of RNase II and evidence for efficient degradation in an *ams pnp rnb* mutant. *EMBO J.* **13**:14, 3368-3377.

Huang, D.B., A. Mohanty, H.L. DuPont, P.C. Okhuysen and T. Chiang, 2006. A review of an emerging enteric pathogen: enteroaggregative *Escherichia coli*. *J. Med Microbiol.* **55**:10 1303-1311.

Ishii, S. and M. J. Sadowsky, 2009. Applications of the rep-PCR DNA fingerprinting technique to study microbial diversity, ecology and evolution. *Env. Microbiol.* **11**: 4, 733-740.

Jay, J. M., 2000. Modern Food Microbiology. *Aspen Publishers, Inc.*, Gaithersburg, MD.

Leung, B. O., F. Jalilehvand and R. K. Szilagy, 2008. Electronic structure of transition metal-cysteine complexes from x-ray absorption spectroscopy. *J. Phys. Chem.* **112**: 15, 4770-4778.

Lisdat, F. and D. Schafer, 2008. The use of electrochemical impedance spectroscopy for biosensing. *Anal. Bioanal. Chem.* **391**, 1555-1567.

Liu, Y., Y. Wang, J. Jin, H. Wang, R. Yang and W. Tan, 2009. Fluorescent assay of DNA hybridization with label-free molecular switch: reducing background-signal and improving specificity by using carbon nanotubes. *Chem. Commun.* **6**, 665-667.

- Mallin, M. A., K. E. Williams, E. C. Esham and r. P. Lowe, 1999. Effect of human development on bacteriological water quality in coastal watersheds. *Ecol. Appl.* **10**, 1047-1056.
- Meays, C. L., K. Broersma, R. Nordin and A. Mazumder, 2004. Source tracking fecal bacteria in water: a critical review of current methods. *J. of Env. Management*, **73**:1, 71-79.
- Mejri, M. B., H. Baccar, E. Baldrich, F. J. Del Campo, S. Helali, T. Ktari, A. Simonian, M. Aouni and A. Abdelghani, 2010. Impedance biosensing using phages for bacteria detection: generation of dual signals as the clue for in-chip assay confirmation. *Biosensors and Bioelectronics*. **26**: 4, 1261-1267.
- Messing, D. S., A. L. Ghindilis and K. Schwarzkopf, 2010. Impedimetric biosignal analysis and quantification in a real-time biosensor system. *IEEE EMBS Conference*, Buenos Aires, Argentina.
- Oregon DEQ, 2012. Monitoring toxic pollutants in the Willamette River basin. Oregon Department of Environmental Quality, Laboratory & Environmental Assessment Division, Hillsboro, OR. 10pp.
- Perna, N. T., G. Plunkett III, V. Burland, B. Mau, J. D. Glasner, D. J. Rose, G. F. Mayhew, P. S. Evans, J. Gregor, H. A. Kirkpatrick, G. Posfai, J. Hackett, S. Klink, A. Boutin, Y. Shao, L. Miller, E. J. Groteck, N. W. Davis, A. Lim, E. T. Dimalanta, K. D. Potamouisis, J. Apodaca, T. S. Anantharaman, J. Lin, G. Yen, D. C. Schwartz, R. A. Welch and F. R. Blattner, 2001. Genome sequence of enterohaemorrhagic *Escherichia coli* O157:H7. *Nature* **409**, 529-533.
- Rodriguez-Mozaz, S., M. P. Marco, J. Lopez de Alda and D. Barcelo, 2004. Biosensors for environmental applications: future development trends. *Pure and Appl. Chem.* **76**: 4, 723-752.
- Scholin, C. A., G. Doucette, S. Jensen, B. Roman, D. Pargett, R. Marin III, C. Preston, W. Jones, J. Feldman, C. Everlove, A. Harris, N. Alvarado, E. Massion, J. Birch, D. Greenfield, R. Vrijenhoek, C. Mikulski and K. Jones, 2009. Remote detection of marine microbes, small invertebrates, harmful algae and biotoxins using the environmental sample processor (ESP). *Oceanography* **22**: 2, 158-167.
- Scholin, C.A., 2009. What are “ecogenomic sensors?” – a review and thoughts for the future. *Ocean Sci. Discuss.* **6**, 191-213.
- Sen, K. and N. J. Ashbolt, 2011. Environmental microbiology: current technology and water applications. *Caister Academic Press*, Norfolk, UK.
- Shanks, O.C., C. Nietch, M. Simonich, M. Younger, D. Reynolds, and K.G. Field, 2006. Basin-wide analysis of the dynamics of fecal contamination and fecal source identification in Tillamook Bay, Oregon. *Applied and Environ. Microbiol.* **72**: 5537-5546
- Skladal, P., 1997. Advances in electrochemical immunosensors. *Electroanalysis*, **9**: 10, 737-745.
- Tokarsky, O. and D. L. Marshall, 2008. Immunosensors for rapid detection of *Escherichia coli* O157:H7- Perspectives for use in the meat processing industry. *Food Microbiol.* **25**: 1, 1-12.

USGS, 2013. Description of Columbia River and Puget Sound Basins. <http://pubs.usgs.gov/sir/2007/5186/section3.html>. Accessed July 4, 2013.

Wagner, M., H. Schmidt, A. Loy and J. Zhou, 2007. Unravelling microbial communities with DNA-microarrays: challenges and future directions. *Microbiol. Ecol.* **53**, 498-506.

Wang, J., G. Rivas, X. Cai, E. Palecek, P. Nielsen, H. Shiraishi, N. Dontha, D. Luo, C. Parrado, M. Chicharro, P.A.M Farias, F.S. Valera, D.H. Grant, M. Ozsoz and M.N. Flair, 1997. DNA electrochemical biosensors for environmental monitoring. *Analytica Chimica Acta* **347**:1-2, 1-8.

Welch, R. A., V. Burland, G. Plunkett III, P. Redford, P. Roesch, D. Raskos, e. L. Buckles, S. R. Liou, A. Boutin, J. Hackett, D. Stroud, G. F. Mayhew, D. J. Rose, S. Zhou, D. C. Schwartz, N. T. Perna, H. L. T. Mobleys, M. S. Donnenberg and F. R. Blattner, 2002. Extensive mosaic structure revealed by the complete genome sequence of uropathogenic *Escherichia coli*. *PNAS* **99**: 26, 17020-17024.

Wirth, T., D. Falush, R. Lan, F. Colles, P. Mensa, L. H. Wieler, H. Karch, P. R. Reeves, M. C. J. Maiden, H. Ochman and M. Achtman, 2006. Sex and virulence in *Escherichia coli*: an evolutionary perspective. *Molec. Microbiol.* **60**: 5, 1136-1151.

Zhang, J., P. Chen, X. Wu, J. Chen, L. Xu, G. Chen and F. Fu, 2011. A signal-on electrochemiluminescence aptamer biosensor for the detection of ultratrace thrombin based on junction-probe. *Biosensors and Bioelectronics* **26**: 5, 2645-2650.